DOI:10.14753/SE.2025.3164

SEMMELWEIS EGYETEM

DOKTORI ISKOLA

Ph.D. értekezések

3164.

KÉCSÁN-RÉVÉSZ CSABA

Kórélettan és transzlációs medicina

című program

Programvezető: Dr. Benyó Zoltán, egyetemi tanár

Témavezetők: Dr. Hamar Péter, egyetemi tanár

Dr. Szénási Gábor, tudományos főmunkatárs

DOI:10.14753/SE.2025.3164

THE ROLE OF OXIDATIVE STRESS ENZYMES AND THE MARKERS OF ISCHEMIC ACUTE KIDNEY INJURY IN MICE

PhD thesis

Csaba Kécsán-Révész

Semmelweis University Doctoral School

Theoretical and Translational Medicine Division

Supervisors:	Péter Hamar, MD, D.Sc Gábor Szénási, C.Sc
Official reviewers:	András Garami, MD, D.Sc Domonkos Pap, MD, Ph.D
Head of the Complex Examination Committee:	Alán Alpár, MD, D.Sc
Members of the Complex Examination Committee:	Miklós Kellermayer, MD, D.Sc Mihály Kovács, D.Sc

Budapest
2025

DOI:10.14753/SE.2025.3164

Table of Contents

DOI:10.14753/SE.2025.3164

DOI:10.14753/SE.2025.3164

List of Abbreviations

ANOVA	analysis of variance
AKI	acute kidney injury
APC	apocynin
ARF	acute renal failure
ATI	acute tubular injury
ATN	acute tubular necrosis
ATP	adenosine triphosphate
BUN	blood urea nitrogen
BSA	bovine serum albumin
BW	body weight
Ca	calcium
CaM	calmodulin
cDNA	complementary DNA
CKD	chronic kidney disease
Cr	creatinine
Cre	Cre recombinase (derived from the P1 bacteriophage)
Cys-C	cystatin C
DAB	3,3'-diaminobenzidine
Dbl	diffuse B-cell lymphoma
DH	Dbl family-homolog
DNA	deoxyribonucleic acid
DPI	protein disulfide isomerase
dsDNA	double-stranded DNA
DT	double treatment
DUOX1	dual oxidase 1
DUOX2	dual oxidase 2
DUOXA1	dual oxidase activator 1
DUOXA2	dual oxidase activator 2
EDTA	ethylenediaminetetraacetic acid
ELISA	enzyme-linked immunosorbent assay

EMR1	epidermal growth factor-like module-containing mucin-like hormone receptor-like 1 (F4/80)
ER	endoplasmic reticulum
F4/80	alias of EMR-1 (epidermal growth factor-like module-containing mucin-like hormone receptor-like 1)
FACS	fluorescence-associated cell sorting
FAD	flavin adenine dinucleotide
Fe-S	iron-sulfur cluster
FFPE	formalin-fixed paraffin-embedded
fLcn2	filtered lipocalin-2
flox	flanked DNA sequence/gene with loxP sites
fw	forward
GAPDH	glyceraldehyde-3-phosphate dehydrogenase
GFR	glomerular filtration rate
GPX3	glutathione peroxidase 3
H_2O_2	hydrogen peroxide
HDI	hydrodynamic injection
HE	hematoxylin-eosin
HIER	heat-induced epitope retrieval
HO-1	heme oxygenase 1
HRP	horseradish peroxidase
Hsp	heat shock protein
Hsp70	70kDa heat shock protein
Hsp90	90 kDa heat shock protein
IHC	immunohistochemistry
IgG	immunoglobulin G
Il-1, -6, -8	interleukin-1, -6, -8
i.p.	intraperitoneal
i.v.	intravenous
I/R	ischemia-reperfusion
IRI	ischemia-reperfusion injury
KDIGO	Kidney Disease: Improving Global Outcomes

KIM1	kidney injury molecule-1
Lcn2	lipocalin-2 (NGAL)
L-FABP	liver-type fatty acid-binding protein
Ly6G	lymphocyte antigen 6 complex, locus G
LyzM	lysozyme M
Mcl-1	myeloid cell leukemia sequence 1
Mcl-1$^{\Delta Myelo}$	Mcl1$^{flox/flox}$LysM$^{Cre/Cre}$ mutants characterized by myeloid-specific conditional deletion of Mcl-1
MCP-1	monocyte chemoattractant protein-1
MPO	myeloperoxidase
miRNA	micro RNA
Mito	mitochondrion
Moco	molybdenum cofactor
mRNA	messenger RNA
NADPH	nicotinamide adenine dinucleotide phosphate
NAG	N-acetyl-β-D-glucosamininidase
NC	non-coding
NCBI	National Center for Biotechnology Information
NGAL	neutrophil gelatinase-associated lipocalin (Lcn2)
non-op	non-operated
NOS	nitric oxide synthase
NOX	NADPH oxidase
NOX1	NADPH oxidase 1
NOX2	NADPH oxidase 2
NOX3	NADPH oxidase 3
NOX4	NADPH oxidase 4
NOX5	NADPH oxidase 5
NOXA1	NADPH oxidase activator 1
NOXO1	NADPH oxidase organizer 1
NRF2	nuclear factor erythroid 2-related factor 2
OXP	oxypurinol
p22^{phox}	22kDa protein subunit of phagocyte oxidase

	(alpha chain of cytochrome b_{558})
$p40^{phox}$	40kDa protein subunit of phagocyte oxidase
$p47^{phox}$	47kDa protein subunit of phagocyte oxidase
$p67^{phox}$	67kDa protein subunit of phagocyte oxidase
PAS	periodic acid-Schiff
PCD	programmed cell death
PCR	polymerase chain reaction
PDI	protein disulfide isomerase
PIP	phosphatidylinositol phosphate
pLcn2	plasma lipocalin-2
Poldip2	type 2 polymerase delta interaction protein
PM	plasma membrane
PMN	polymorphonuclear
qPCR	quantitative polymerase chain reaction
Rac	Ras-Related C3 Botulinum Toxin Substrate 1
	(rho family small GTP binding protein)
rev	reverse
RNA	ribonucleic acid
RNAi	RNA interference
ROS	reactive oxygen species
s.c.	subcutaneous
sCr	serum creatinine
SEM	standard error of the mean
sham-op	sham-operated
siNC	non-coding siRNA
siNOX2	NADPH oxidase 2 siRNA
siNOX4	NADPH oxidase 4 siRNA
siRNA	short interfering RNA
siXOR	xanthine oxidoreductase siRNA
TBS	Tris-buffered saline
TEC	tubular epithelial cell
TKS4/5	Src3 homology domain tyrosine kinase substrate 4/5

TLR4	toll-like receptor 4
TMB	3,3',5,5'-tetramethylbenzidine
TMA	tissue microarray
TNFα	tumor necrosis factor alpha
Tris	tris(hydroxymethyl)aminomethane
uCr	urinary creatinine
uLcn2	urinary lipocalin-2
VEH	vehicle
WT	wild type/wild-type
XDH	xanthine dehydrogenase
XO	xanthine oxidase
XOR	xanthine oxidoreductase

DOI:10.14753/SE.2025.3164

1. INTRODUCTION

1.1. Acute Kidney Injury

1.1.1. Definition

Acute kidney injury (AKI, formerly known as acute renal failure, ARF) is a rapid, sudden loss of kidney function and is associated with poor clinical outcomes, representing a severe problem in clinical nephrology (1, 2). The *2012 Clinical Practice Guideline*, prepared and released by *Kidney Disease: Improving Global Outcomes* (KDIGO), established standard criteria for AKI that are currently in use (3). An update for the *2012 Clinical Practice Guideline for Acute Kidney Injury* is under development but has not yet been published by KDIGO. AKI is defined as an increase in serum creatinine (sCr) of ≥26.5 μmol/L (0.3 mg/dL) within 48 hours or an increase of ≥1.5 times baseline value within 7 days or urine volume <0.5 mL/kg/h (oliguria) for ≥6 hours (3).

1.1.2. Incidence and Types

The incidence of AKI is approximately 5% to 20% among hospitalized patients and 20% to 50% among intensive care unit patients (4-7). These data on the incidence of AKI vary by population, public health services, national income, and economic status of countries.

Based on its primary etiology, AKI can be categorized into three types: prerenal, intrarenal, and postrenal (6, 8). AKI can develop due to prerenal factors, such as circulatory shock, cardiac failure, or hepatorenal syndrome. Additionally, perioperative and hospital-acquired AKI can result from vascular, hepatic, or cardiac surgeries. The underlying cause of prerenal AKI is a decrease in the glomerular filtration rate (GFR) caused by hypoperfusion, which leads to structural renal damage. Frequently, AKI may have an intrarenal etiology through renal parenchymal lesions caused by nephrotoxicity, sepsis, trauma, or ischemia. Kidney transplantation is invariably accompanied by ischemia-reperfusion (I/R) injury (IRI), which is challenging to prevent during the transplantation procedure. The third class of AKI has a postrenal cause primarily related to obstruction of the urinary tract, often due to prostatic hyperplasia or prostate cancer. Furthermore, AKI itself may contribute to the pathology of chronic kidney disease (CKD), as it is increasingly recognized that AKI might lead to CKD (9).

DOI:10.14753/SE.2025.3164

1.2. Renal Ischemia-Reperfusion Injury

1.2.1. Pathomechanism

IRI is one of the leading causes of AKI (10). IRI involves various pathophysiological mechanisms, including tubular and vascular dysfunction due to oxidative stress-induced epithelial and endothelial cell injuries, concomitant inflammation, and multiple types of cell death, resulting in structural and functional renal damage (11).

1.2.1.1. Ischemia

Ischemia occurs when blood flow is reduced or blocked in a specific supply region (Fig. 1). The decreased or interrupted oxygen and nutrient delivery leads to disturbed energy metabolism and a shift to anaerobic metabolism (12). Hypoxia disrupts the electron transport chain in mitochondria, and the intracellular ATP drops (13). Dysfunction of the membrane-bound ion pump activity leads to metabolic acidosis, impaired enzyme function, and redox imbalances (14). The compromised enzyme activities lead to decreased antioxidant capacity. Due to the cessation of the activity of redox enzymes, only a minimal amount of reactive oxygen species (ROS) is produced during renal ischemia.

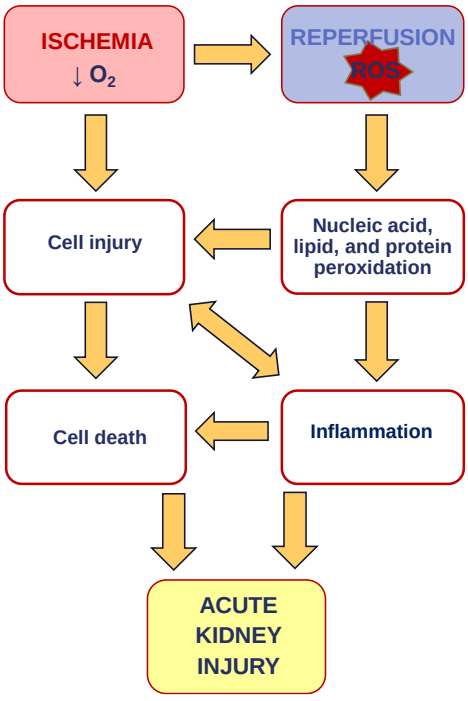

Figure 1. The schematic diagram illustrating the pathomechanism of ischemia-reperfusion injury. ROS: reactive oxygen species.

1.2.1.2. Reperfusion

Reintroducing oxygen to the ischemic tissue by restoring blood flow facilitates recovery of the oxygen-deficient region (Fig. 1). During reperfusion, the ROS production increases explosively, which, combined with reduced antioxidant capacity, promotes a secondary renal tissue injury during the reperfusion (reperfusion injury) (15). The most common oxygen radicals are superoxide ($O_2^{\bullet-}$), hydroxyl ($^{\bullet}OH$), peroxyl ($RO_2^{\bullet}$), alkoxyl ($RO^{\bullet}$), peroxynitrite ($ONOO^-$), hypochlorite anion ($HOCl^-$), and hypochlorite (ClO^-) (16, 17). Non-radical derivatives, such as hypochlorous acid (HOCl), ozone (O_3), singlet oxygen ($^1O_2$), and hydrogen peroxide (H_2O_2), are oxidizing agents themselves or can be easily converted into radicals (16, 17). ROS-driven oxidative stress primarily damages the cellular biomolecules (lipids, proteins, and nucleic acids), causing membrane disintegration, cytoskeletal integrity disruption, enzyme dysfunction, and DNA and mitochondria fragmentation (12, 13, 15).

1.2.1.3. Inflammation

The ROS-induced epithelial and endothelial cell injuries result in the accumulation of toxic byproducts, namely damage-associated molecular patterns (DAMPs), which initiate leukocyte infiltration accompanied by cytokine release (10). The innate inflammatory response aggravates oxidative damage (Fig. 1). The endothelial dysfunction manifests as increased capillary permeability and an imbalance between dilator and constrictor vasoactive factors. An increase in vascular permeability enhances the extravasation of leukocytes through the endothelium (18). Inflammation of the damaged capillary walls leads to platelet activation, blood coagulation, impaired flow, and microvascular occlusions (11, 19). Both activated endothelial cells and polymorphonuclear (PMN) granulocytes are significant ROS sources in the postischemic kidney (20). The infiltrating leukocytes, principally PMN granulocyte neutrophils and mononuclear monocyte macrophages, exacerbate the primary injury, causing inflammation in the injured tissue. Injured tubular epithelial cells produce various factors, including interleukins (Il-1, Il-6, Il-8), tumor necrosis factor-1 (TNFα), and monocyte chemoattractant protein-1 (MCP-1), promoting leukocyte infiltration. Recruited leukocytes release Il-1, Il-8, MCP-1, and ROS, creating a positive loop, promoting inflammation and, thus, exacerbating renal injury (8). However, the phagocytic immune cells also contribute to tissue repair (21-23).

1.2.1.4. Cell Death

The I/R-induced extensive and severe cellular injury can lead to necrosis of the postischemic renal tissue (Fig. 1). Depending on the extent of I/R-induced injury to cellular components, various programmed cell death (PCD) pathways are activated in the postischemic kidney, including apoptosis, necroptosis, pyroptosis, and ferroptosis. The histological manifestation of IRI is acute tubular necrosis (ATN), but the term acute tubular injury (ATI) is also used in the histological assessment of morphological changes in the injured tubules. Depending on the severity of the postischemic injury, various signs of tubular epithelial cell damage are present in ATI, including loss of brush border, dilation of tubules, cast formation, and different forms of cell death (24).

1.3. Ischemic Acute Kidney Injury

1.3.1. Pathophysiology

The formation of concentrated urine in the kidney is based on the countercurrent mechanism, which results in the medulla having a physiologically low oxygen tension. If hypoperfusion occurs from prerenal causes, renal autoregulation of the afferent and efferent arterioles maintains GFR, which reduces blood flow to the medulla, causing a lower oxygen tension (25). Due to the highly oxygen-demanding, energy-intensive transport function of tubules, reduced oxygen supply to the renal parenchyma leads to severe ischemia in the medulla, where the oxygen concentration in the vasa recta is the lowest (26). Reduced oxygen supply affects the tubular epithelial cells (TECs). Besides the TECs of the medulla, mainly the proximal tubular epithelial cells (PTECs) are affected as 70% of the energy (ATP) and oxygen-demanding active transport is in the proximal tubules, which are located in the S3 segment of the outer medulla (26). I/R-induced injury to TECs leads to tubular necrosis in the renal parenchyma. As described, ATN is the most pronounced in the medulla, specifically in the S3 segments of the PTECs (skip lesion), which are the most vulnerable parts of the kidney to IRI (26, 27). Hypovolemia and hypoperfusion activate the renin-angiotensin-aldosterone system (RAAS) and the sympathetic nervous system, each of which constricts the afferent and efferent arterioles and decreases the medullary microcirculation by constriction of the vasa recta (27). Thus, reducing glomerular filtration results in glomerular and medullary microcirculatory hypoperfusion. Microcirculatory ischemia damages endothelial cells (ECs), causing

functional impairment in response to vasoactive substances and increasing endothelial permeability, which promotes leukocyte adherence, inflammation, and ROS production. While persistent vasoconstriction initiates microcirculatory impairment and EC injury, consequent capillary occlusion due to endothelial-leukocyte interactions and activation of the coagulation system leads to microcirculatory insufficiency, exacerbating ischemia (26). Endothelial injury with inflammation and coagulation, combined with attenuated vascular relaxation after reperfusion due to endothelial dysfunction, resulted in a "no-reflow phenomenon" in the IRI-affected blood vessels (28).

1.3.2. Key Principles of the Pathophysiology Based on the Severity of Acute Kidney Injury

When I/R leads to AKI, its severity is proportional to the duration of the ischemic period. Only mild parenchymal injury occurs if ischemia is of short duration, and the functional decline is generally reversible (Fig. 2A). I/R-induced mild AKI (6) is characterized by a mild, often transient, decrease in excretory function and urine output. Mild AKI is accompanied by minimal cell necrosis or loss. The subsequent nephron number is maintained, and no permanent adaptative cellular responses are required. The insignificant nephron loss results in a mild or subclinical decrease in total GFR as a long-term outcome. The cells most sensitive to hypoxia are the tubular epithelial cells (TECs), which can regenerate from tubular epithelial stem cells aided by the paracrine support of hematopoietic stem cells, which facilitates healing (26).

Longer ischemia leads to moderate AKI (6) when nephron loss is more pronounced, and the total GFR is clinically reduced (Fig. 2B). The regeneration from clonal expansion of the progenitor cells in the injured tubules leads to partial restoration of the renal structure and function (29). However, some TECs cannot recover and become necrotic. The tubules, in which damaged segments cannot heal, undergo atrophy and are irreversibly lost. Necrosis is accompanied by acute necroinflammation, where oxidative damage and inflammation are enhanced in an autoamplification loop (30). The long-term outcomes of moderate AKI are 1: compensatory hypertrophy of the remnant nephrons leading to an increase in single-nephron GFR, and 2: the residual structural and functional damage resulting in a significant decrease in total GFR (6).

DOI:10.14753/SE.2025.3164

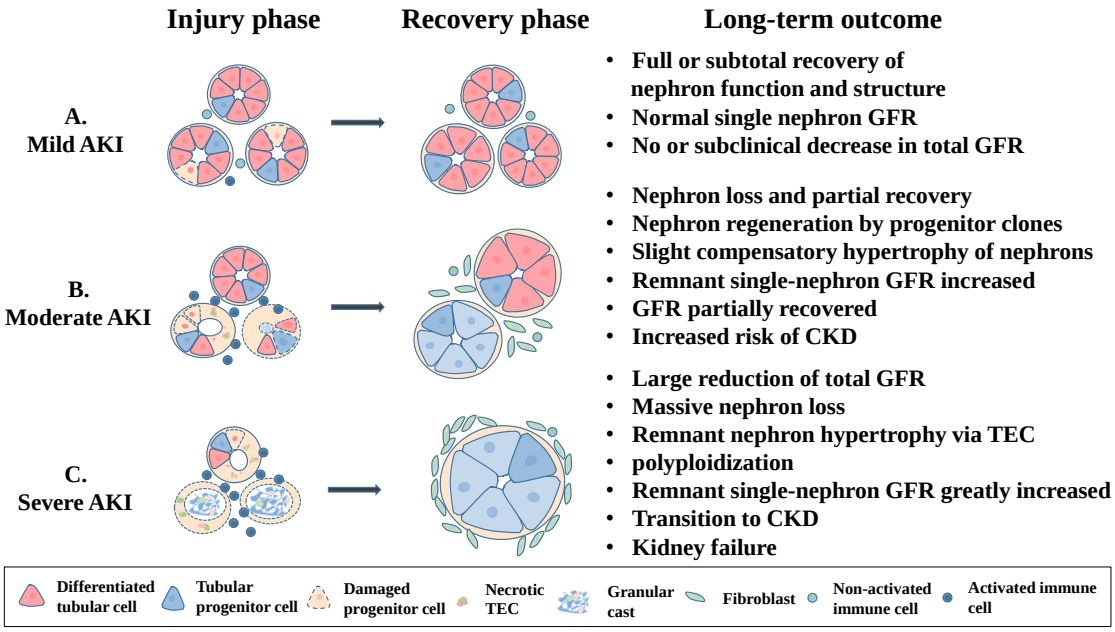

Figure 2. Main principles of the pathophysiology according to the severity of acute kidney injury (AKI). (A) Mild AKI, (B) Moderate AKI, (C) Severe AKI. GFR: glomerular filtration rate; CKD: chronic kidney disease; TEC: tubular epithelial cell. Figures based on Kellum JA et al. (6).

Severe AKI (6), caused by a long-lasting ischemic event, is characterized by massive nephron loss due to extensive necrosis (Fig. 2C). Tubule repair occurs only in nephrons where surviving progenitor cells are present. Fibrotic tissue forms in place of the atrophized nephrons, stabilizing the structural integrity of the remaining nephrons. Massive irreversible loss of nephrons reduces kidney lifespan. Nephron loss forces an increase in the functional capacity of the preserved nephrons to adapt to metabolic demand. The compensatory process in remaining nephrons results in secondary glomerular damage (31). This adaptation to hyperfiltration is accomplished by increasing the size of the remnant nephrons. The increase in glomerular size is accompanied by tubular enlargement through TEC polyploidization, resulting in massive nephron enlargement (6). Enlarged nephrons characterize the histology of a severely damaged kidney after recovery. Single-nephron GFR increases significantly in the enlarging, hyperfiltrating remnant nephrons. Nephron hypertrophy frequently exceeds the adaptive capacity of podocytes. This consequent podocyte dysfunction leads to secondary focal segmental glomerulosclerosis and subsequent loss of the preserved nephrons, facilitating a transition to CKD (32).

1.4. Oxidative Stress in Ischemia-Reperfusion

1.4.1. Redox Homeostasis After Ischemia-Reperfusion

Excessive production of ROS due to ischemia-reperfusion (I/R) is widely considered to be the primary cause of ischemia-reperfusion injury (IRI). Under normal physiological conditions, the tight regulation of ROS generation and removal maintains redox homeostasis in a dynamic equilibrium (33). Various enzymatic and non-enzymatic antioxidant systems are essential for maintaining the delicate balance between generating and eliminating ROS. Enzymes of the antioxidant system include superoxide dismutase, catalase, peroxidases, paraoxonase, glutathione S-transferase, glutathione peroxidase, and thioredoxin (34, 35). The non-enzymatic components include cysteine, glutathione, carotenoids, retinol, ascorbate, and α-tocopherol (34, 35). Together, these systems play a vital role in the defense against oxidative stress.

During ischemia, the reduction of oxygen supply leads to the transition to anaerobic metabolism. Disruption of redox enzyme activity results in intermittent ROS production during ischemia. However, restoration of oxygen during reperfusion accelerates ROS production, which, combined with reduced antioxidant capacity, throws off the balance of redox homeostasis. This redox imbalance increases oxidative stress and contributes to tissue injury (15). Various enzymes can produce ROS under physiological and pathological conditions. Enzyme families, including mitochondrial respiratory enzymes, lipoxygenase, xanthine oxidase, and cyclooxygenase, and enzymes of the nicotinamide adenine dinucleotide phosphate oxidase (NADPH oxidase, NOX) family are responsible for ROS production (36, 37). The NOX family enzymes are unique in that their only function is to generate ROS, whereas the other listed enzymes produce ROS as a byproduct.

1.4.2. NADPH Oxidase Family

1.4.2.1. Structure and Function

Enzymes of the NOX family (NOX1-5 and DUOX1-2) are multi-subunit enzymes with membrane-bound (catalytic, including $gp91^{phox}$-$p22^{phox}$) and cytosolic (regulatory, including $p47^{phox}$, $p67^{phox}$, and $p40^{phox}$) subunits (17).

The NADPH oxidases share a common feature: electron transfer through a conserved transmembrane catalytic domain (38). In this process, NADPH is the electron donor,

while molecular oxygen is the acceptor. As a result of this reaction, oxygen is converted into superoxide anion or hydrogen peroxide.

All family members have an NADPH-binding and a flavin adenine dinucleotide (FAD)-binding domain in the C-terminal part, which extends into the cytosol. Towards the N-terminus is a region of six α-helical transmembrane domains. The transmembrane region contains four conserved histidines that bind two prosthetic heme groups, which are essential for transmembrane electron transport. Specific NOX isoforms consist of further domains, including intracellular calcium-binding "EF-hand" motifs, extracellular peroxidase-homolog domain, and an additional transmembrane domain.

1.4.2.2. NOX2

The first described member of the enzyme family was $gp91^{phox}$ (NOX2) from PMN phagocytes, and the family members are classified by their shared sequence homology with $gp91^{phox}$ (39).

NOX2 forms an enzyme complex (Fig. 3B) with another transmembrane protein, $p22^{phox}$, to create flavocytochrome b_{558} (40). Moreover, $p22^{phox}$ is essential in building complexes with NOX1-4 isozymes (41). $p22^{phox}$ contains two transmembrane regions with heme-binding histidines and a cytosolic $p47^{phox}$-binding (NOXO1-binding) domain (42). Activation of the $gp91^{phox}$-$p22^{phox}$ complex occurs by binding the cytosolic regulatory subunits, $p47^{phox}$, $p67^{phox}$, and $p40^{phox}$, to the membrane-bound structure. Subsequently, the enzyme complex is completed by adding a GTP-binding Rac protein, thus finalizing the active complex.

NOX2 was primarily identified in phagocyte PMNs (43, 44). Its primary function is to serve as an immune response effector that generates oxidative bursts to eliminate pathogens. Recent studies indicate that NOX2 is also widely expressed in non-phagocytic cells in a variety of tissues (including cardiomyocytes, skeletal muscle, smooth muscle, endothelium, hepatocytes, neurons, hematopoietic stem cells (17)), where it plays a role in signal transduction, angiogenesis, and cell death (45).

DOI:10.14753/SE.2025.3164

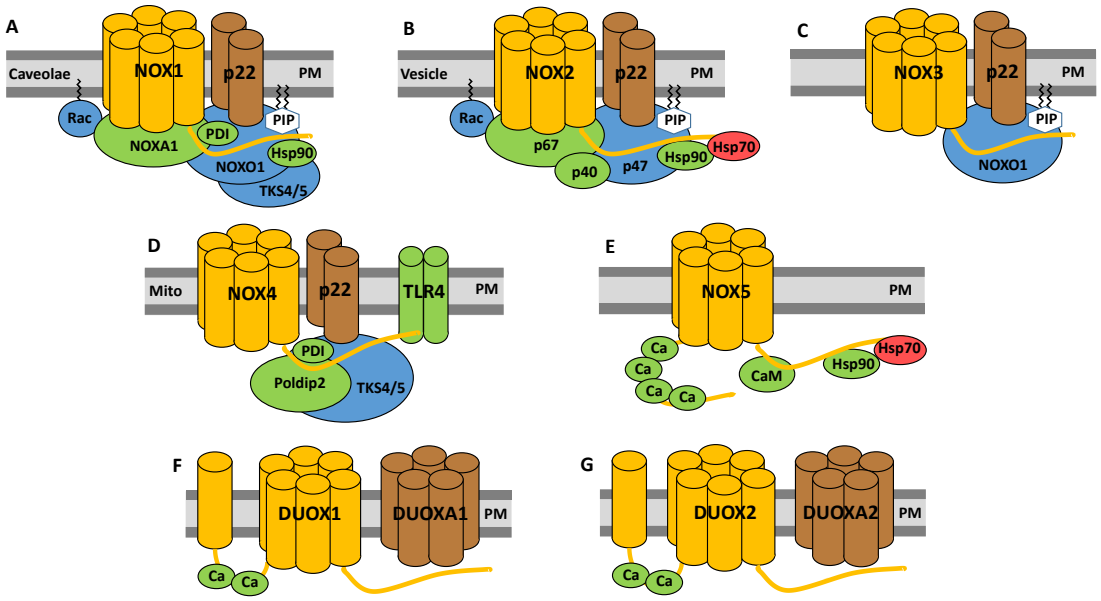

Figure 3. The NADPH oxidase enzyme family. (A) NADPH oxidase 1 (NOX1), (B) NADPH oxidase 2 (NOX2), (C) NADPH oxidase 3 (NOX3), (D) NADPH oxidase 4 (NOX4), (E) NADPH oxidase 5 (NOX5), (F) Dual oxidase 1 (DUOX1), (G) Dual oxidase 2 (DUOX2), p22: 22 kDa protein subunit, p40: 40 kDa protein subunit, p67: 67 kDa protein subunit, NOXA1: NOX activator 1, NOXO1: NOX organizer 1, Rac: Ras-related C3 botulinum toxin substrate 1, PDI: protein disulfide isomerase, PIP: phosphatidylinositol phosphate, Hsp70: heat shock protein 70, Hsp90: heat shock protein 90, TKS4/5: tyrosine kinase substrate with 4/5 SH3 domains, Poldip 2: polymerase (DNA-directed) delta-interacting protein 2, DUOXA1-2: dual oxidase activator 1-2, TLR4: Toll-like receptor 4, Ca: calcium, CaM: calmodulin, PM: plasma membrane, Mito: mitochondrion. Based on the paper of Altenhofer S et al. (46).

1.4.2.3. NOX4

The kidney-specific homolog of $gp91^{phox}$ is the NOX4 isoform (47). Due to its predominant renal localization, NOX4 is also known as Renox. NOX4 is also expressed in adipose tissue, endometrium, breast, heart muscle, osteoclasts, hematopoietic stem cells, keratinocytes, neurons, and thyroid (17). Its primary cellular localization is the mitochondrial membrane and the endoplasmic reticulum (ER) (48, 49).

Similar to NOX1-3, NOX4 (Fig. 3D) contains six transmembrane domains forming two intracellular loops and three extracellular loops (labeled A-E), with the outer E loop being longer and involved in H_2O_2 production (50). At the cytosolic C-terminal, a DH domain contains a FAD- and a NADPH-binding site, which are essential for the catalytic

activity. As in NOX1-3, there are four conserved, heme-binding histidines in the transmembrane region.

A characteristic functional feature of NOX4 is its constitutive activity, which is vital in the regulation of fluid balance as an oxygen and sodium sensor (51). Thus, its constitutively active function makes it a crucial element in maintaining fluid homeostasis. NOX4 does not require cytosolic regulatory components for its function; it requires only $p22^{phox}$ to assemble and maintain a constitutively active complex (52). Another unique feature of NOX4 is that it mainly produces H_2O_2, in addition to $O_2^{\bullet-}$. Superoxide dismutation converts $O_2^{\bullet-}$ into H_2O_2 and O_2. Whether H_2O_2 vs. $O_2^{\bullet-}$ releases as a product is thought to be influenced by the intrinsic rapid dismutation of $O_2^{\bullet-}$ in the complex before it leaves it (50). The production of H_2O_2 is considered a double-edged sword; H_2O_2 can be vasoprotective as a second messenger regulating transcription factors in various signaling pathways but can cause oxidative damage as a ROS product (53, 54).

1.4.2.4. Other NADPH Oxidase Isoforms

NOX1 is the first identified homolog of $gp91^{phox}$ (55). This isoform (Fig. 3A) is mainly expressed in the colon epithelial and vascular smooth muscle cells and is also found in the uterus, placenta, and prostate (17, 55). Its primary function is host defense in the colon (56) and vascular regulation and angiogenesis in the vessels (57, 58).

NOX3 is exclusively present in the inner ear of postnatal tissues (59). Genetic lack of NOX3 resulted in vestibular disorder in mice (60). NOX1- or NOX3-associated enzyme complexes are assembled with NOXO1, NOXA1, and small GTPase Rac subunits to form a functional complex (Fig. 3C) (61).

NOX5 is a distant homolog of $gp91^{phox}$ (62), which has been lost evolutionarily in rodents (63). Unlike NOX1-4, NOX5 (Fig. 3E) does not require $p22^{phox}$ for stabilization nor cytosolic subunits to attain active conformation (61). Moreover, this isoform contains intracellular "EF-hand" motifs in addition to the shared, conserved domains and is regulated in a calcium-dependent manner (64). NOX5 is expressed mainly in the spleen and testis, as well as in the uterus, endothelium, and placenta (17, 62). NOX5 is thought to play a significant role in sperm capacitation (65).

DUOX1 and 2 (Fig. 3F and 3G) are referred to as dual oxidases because they contain a peroxidase-homolog domain on the extracellular side, along with their NADPH oxidase

domain. Historically, they were named thyroid oxidases due to their primary localization in the thyroid gland. DUOX1 and 2 rely on DUOXA1 és DUOXA2 maturation factors, respectively, to mediate their translocation from ER to the plasma membrane (66, 67). Dual oxidases contain intracellular "EF-hand" motifs, meaning their regulation depends on calcium signals.

Like thyroperoxidase, DUOX2 is found in the apical membrane of thyrocytes and produces H_2O_2 to synthesize thyroid hormones. Lack of DUOX2 leads to severe hypothyreosis. The physiological role of DUOX1 is uncertain, but it is also expressed mainly in the thyroid gland and produces H_2O_2.

1.4.3. Xanthine Oxidoreductase

Xanthine oxidoreductase (XOR) is a widely distributed enzyme from prokaryotes to eukaryotes and evolutionarily has a variety of physiological functions. Its primary role is to break down purine into uric acid. In humans, XOR is widely expressed in various tissues, mainly in the liver and intestine, but it is also found in the kidney, lung, brain, heart, and blood (68, 69).

XOR is a large homodimeric molybdenum flavoenzyme (Fig. 4) containing the following catalyzing domains per subunit: one molybdenum cofactor (Moco), two ferredoxin iron-sulfur clusters (2Fe/S), and one FAD cofactor (70).

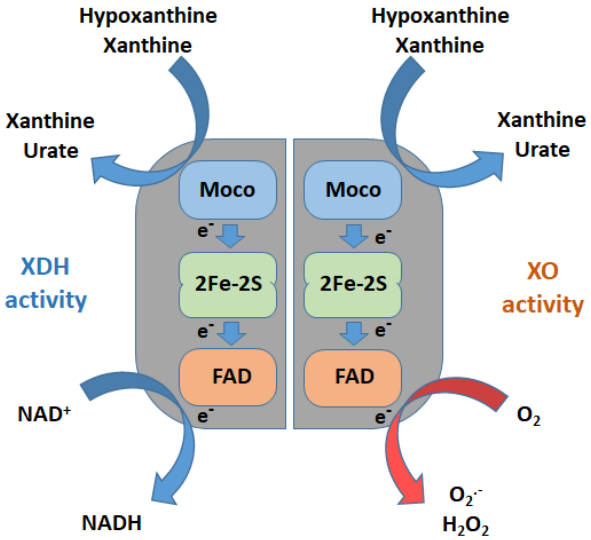

Figure 4. Structure and function of xanthine oxidoreductase. XDH: xanthine dehydrogenase, XO: xanthine oxidase, Moco: molybdenum cofactor, Fe-S: iron-sulfur cluster, FAD: flavin adenine dinucleotide. Figure based on the paper of Harrison R (68).

Moco catalyzes the oxidation of xanthine while the releasing electron flux moves through the Fe/S domain to the FAD site (71, 72). The reduced enzyme is re-oxidized via the FAD activity using NAD^+ or O_2 as an oxidant substrate (73, 74).

The biochemical activities of XOR are as follows (75):

1. Xanthine dehydrogenase (XDH) activity: This performs the final two steps of purine catabolism by catalyzing the oxidation of hypoxanthine to uric acid via xanthine. While converting hypoxanthine into uric acid, XDH reduces NAD^+ to NADH.

2. Xanthine oxidase (XO) activity: In addition to its role in purine catabolism, this activity also produces uric acid from hypoxanthine, but ROS ($O_2^{\bullet-}$ and H_2O_2) are generated from O_2 at the same time.

3. Nitrite reductase activity: This is an alternative NOS-independent nitric oxide production ($^{\bullet}NO$). It produces $^{\bullet}NO$ by reducing NO_2^-, thereby contributing to blood pressure regulation and vasodilatation, a beneficial effect during reperfusion (76).

4. NADH oxidase activity: This activity of XOR also produces ROS ($O_2^{\bullet-}$ and H_2O_2) while oxidizing NADH to NAD^+.

The XOR enzyme is known in two forms in mammals and, thus, in humans: XDH and XO, but they are products of the same gene (77). The enzyme first exists as XDH. Nevertheless, it is readily converted to XO either reversibly by oxidation of specific cysteine residues to form disulfide bridges or irreversibly by limited proteolysis (70). Ischemia is a condition that promotes reversible and partial conversion of XDH to XO (78). This results in a significant change in the redox center at the FAD site accompanied by altered redox properties (70); XOR starts to produce ROS byproducts during reperfusion as it prefers O_2 over NAD^+ as a substrate leading to $O_2^{\bullet-}$ and H_2O_2 products, while catalyzing the hypoxanthine → xanthine → uric acid conversion (Fig. 4 and 5).

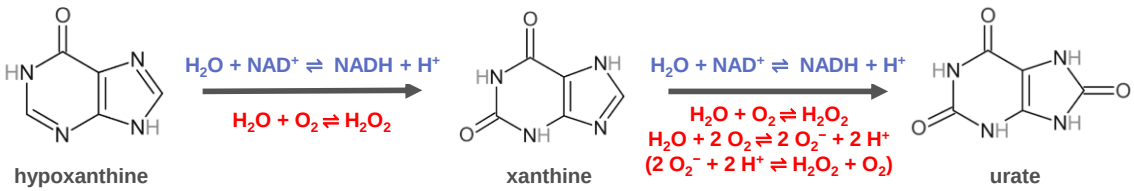

Figure 5. Reactions are catalyzed by the xanthine oxidoreductase enzyme (79, 80). Blue equations: xanthine dehydrogenase activity of the enzyme. Red equations: xanthine oxidase activity of the enzyme. Red in parenthesis: spontaneous reaction.

The preference of O_2 over NAD^+ as the final electron acceptor turns the XO form of XOR into a harmful ROS producer, which can contribute to the I/R pathomechanism by causing oxidative stress through excessive ROS production.

1.4.4. Sources of Reactive Oxygen Species as Therapeutic Targets

NOXs significantly contribute to oxidative stress caused by postischemic ROS generation (14, 17). However, the extent of their contribution to renal IRI of varying severity is unknown, and the pathological role of the NOX4 isoform is controversial.

NOX or XOR inhibition against IRI may have therapeutic potential. Furthermore, several antioxidants are beneficial against IRI (12, 81). However, despite extensive research on inhibiting ROS sources in I/R, its successful translation into clinical therapy for preventing or treating AKI has not been accomplished.

1.5. Biomarkers for Renal Ischemia-Reperfusion Injury

1.5.1. Functional and Injury Markers of Acute Kidney Injury

The most commonly used markers of kidney function with clinical relevance are creatinine (Cr), cystatin C (Cys-C), and urine volume. They are conventionally used to assess AKI, regardless of its etiology.

However, a wide range of injury biomarkers described to predict AKI can help in early detection, e.g., kidney injury molecule-1 (KIM1), lipocalin-1 (Lcn1, also known as neutrophil gelatinase-associated lipocalin, NGAL), N-acetyl-β-D-glucosamininidase (NAG), interleukin-18 (Il-18) and liver-type fatty acid-binding protein (L-FABP) (82). These new molecular markers enable a more precise understanding of the pathomechanisms, identification of AKI sub-phenotypes, earlier diagnosis, and improved prognosis (83).

An emerging group of biomarkers for predicting and diagnosing AKI are the small non-coding micro RNAs (miRNAs) (84). MiRNAs regulate gene expression at the posttranscriptional level, control cell functions, and direct many cellular processes (85). The list of miRNAs implicated in the development of various types of AKI is growing (86, 87). A subset of them are thought to be involved in ischemic AKI, and some of them are promising early biomarkers for predicting I/R-induced AKI (85, 88).

1.5.2. Lipocalin-2 as a Biomarker in the Pathology of Organ Injuries

Conventional functional markers, like Cr or blood urea nitrogen (BUN), can effectively identify severe AKI. However, they could be more reliable during the early stages of AKI. Other tests of renal tubular function, like urinary specific gravity, rely on hydration status and are therefore challenging to standardize. Thus, there is a critical need for a specific and sensitive marker of tubular injury to detect mild AKI beyond the capability of traditional kidney function markers.

Lcn2 (NGAL), a product of injured distal tubular epithelial cells (89, 90), has been identified as a biomarker of AKI of various etiology (91, 92). It also assesses the severity of kidney damage after kidney transplantation, contrast agent administration, or in patients with severe disease (92-94) and in experimental murine AKI models (88, 92, 95). Lcn2 has 3 isoforms: monomeric (25 kDa), homodimeric (45 kDa), and heterodimeric (135 kDa). Human renal tubular cells produce mainly the monomeric and, to some extent, the heterodimeric form (96).

Unlike urea or creatinine retention, which are markers of the overall excretory function of the kidney, Lcn2 is considered a marker of acute tubular cell injury. Thus, Lcn2 may be more sensitive than urea (92) in ischemia-reperfusion or contrast-induced AKI (97). However, Lcn2 is not an exclusive kidney damage marker as plasma Lcn2 (pLcn2) concentration can increase in patients due to epithelial injury or neutrophil activation (98); however, in the latter case, the dimeric form prevails (96). Moreover, Lcn2 expression increased in humans after intestinal (99) or bronchial (100) epithelial injury, inflammation, or cancer (101). The diversity of Lcn2 sources can make it challenging to identify the underlying pathology. After kidney injury, Lcn2 is mainly excreted into the urine, and only a small amount appears in the plasma (102). Plasma Lcn2 is filtered in the glomeruli and is mainly reabsorbed by the proximal tubules if the tubules function correctly (103). Consequently, tubular injury results in a significant increase in urinary Lcn2 excretion accompanied by a relatively small rise in plasma Lcn2 concentration, whereas pathologies in other organs increase plasma but not urinary Lcn2.

DOI:10.14753/SE.2025.3164

2. OBJECTIVES

The first objective was to study the role of two main enzymatic sources of reactive oxygen species (ROS) in renal injury of varying severity using siRNA-based RNA interference (RNAi) and drug inhibitors, as well as the contribution of polymorphonuclear (PMN) granulocytes, i.e., neutrophils, to ischemia-reperfusion (I/R)-induced acute kidney injury (AKI) using a neutrophil-deficient mouse strain.

The following questions were addressed:

1. How do the expression kinetics of ROS-producing enzymes, including NADPH oxidases (NOXs) and xanthine oxidoreductase (XOR), as well as the kinetics of neutrophil infiltration relate to the progression of AKI induced by I/R?
2. Can inhibiting or silencing XOR protect the kidneys from I/R injury of any severity, whether mild, moderate, or severe?
3. Does the kidney-specific NOX isoform (NOX4) contribute to the pathogenesis of renal I/R injury of any severity?
4. Does neutrophil deficiency prevent the pathogenesis of renal I/R injury of any severity?

The second objective was to evaluate the sensitivity and specificity of lipocalin-2 (Lcn2) as a marker of AKI after renal ischemia-reperfusion injury (IRI) of different severities. Plasma and urine concentration and renal Lcn2 expression were measured and correlated with blood urea retention and morphological changes in mice exposed to renal IRI and compared to those of non-operated and sham-operated mice.

The following questions were addressed:

5. Can the sensitivity of Lcn2 make it a reliable biomarker for detecting subclinical IRI-AKI, which is undetectable using conventional renal injury markers?
6. Can Lcn2 serve as a specific marker to differentiate renal and non-renal injuries?

DOI:10.14753/SE.2025.3164

3. METHODS

3.1. Approval

The experiments were approved by the Workplace Animal Welfare Committee of Semmelweis University and the Pest County Government Office (PE/EA/2202-5/2017). All procedures for animal experiments were carried out according to the Hungarian Act on the Protection and Welfare of Animals and the EU Directive 2010/63/EU.

3.2. Animals

Male C57BL/6 (Charles River, Germany) weighing 25.4±3.8 g had free access to standard rodent chow (Akronom Kft., Budapest, Hungary) and tap water, kept under standard conditions (light/dark cycle of 12/12 hours, relative air humidity between 40 and 70%, and ambient temperature at 22 ± 2°C).

Bone marrow chimeras with a neutrophil-deficient $Mcl1^{flox/flox}LysM^{Cre/Cre}$ hematopoietic system were used for testing the role of neutrophil granulocytes (104, 105). Recipient mice were irradiated with 11.5 Gy of gamma radiation using a ^{137}Cs source and treated with unfractionated bone marrow cells from wild-type (WT) or $Mcl1^{flox/flox}LysM^{Cre/Cre}$ mice (referred to as Mcl-$1^{\Delta Myelo}$) via the tail vein (Fig. 6).

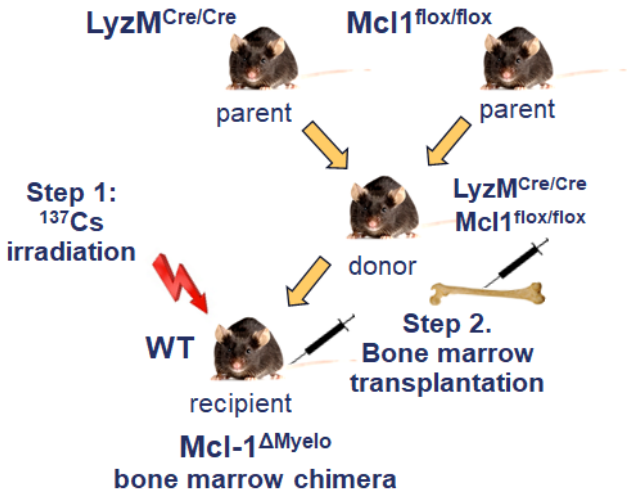

Figure 6. Preparation of the Mcl-$1^{\Delta Myelo}$ bone marrow chimeric, neutrophil functional knockout model. Mcl-1: myeloid cell leukemia 1, LyzM: lysozyme M (coded by Lyz2 gene), Cre: Cre recombinase from P1 bacteriophage, flox: flanked DNA sequence/gene with loxP sites, $Mcl1^{\Delta Myelo}$: $Mcl1^{flox/flox}LysM^{Cre/Cre}$ mutants characterized by myeloid-specific conditional deletion of Mcl-1.

Therefore, Mcl-1$^{\Delta Myelo}$ bone marrow-transplanted mice have a myeloid-specific deletion of Mcl-1 in their bone marrow, which resulted in an inability to generate polymorphonuclear (PMN) neutrophils. Four weeks after bone marrow transplantation, the number of circulating neutrophils isolated from blood samples was counted by flow cytometry. Neutrophils were defined as Ly6G-positive cells within a typical forward and side scatter gate.

Mcl1$^{flox/flox}$LysM$^{Cre/Cre}$ genetic modification was developed on a C57BL/6 background. Breeding of the knockout animals was conducted in the animal house of the Department of Physiology at Semmelweis University. The bone marrow transplantation was performed in the operation suite of the Department of Physiology. The renal ischemia-reperfusion (I/R) operations were carried out in the surgery suite of the Institute of Translational Medicine at Semmelweis University.

3.3. siRNA Application

Lyophilized Stealth™ siRNA (ThermoFisher Scientific, Waltham, MA, USA) pools were used to target NOX4 (Cat Nos.: MSS224870, MSS224872, MSS203388), and XOR (Cat Nos.: MSS238716, MSS238717, MSS278864). Non-coding small interfering RNA (siNC) was used as a negative control. The treatment solutions contained 50 μg of siRNA dissolved in 0.3 ml of sterile physiological saline (Salsol A, Teva, Gödöllő, Hungary) immediately before use. Two days before ischemia, retrograde hydrodynamic injection (HDI) was used to administer siRNA via the left renal vein (106). Briefly, the peritoneum was opened after a midline incision, the aorta was occluded with a clip (BH31, Aesculap, Center Valley, PA, USA) between the origins of the two renal arteries, and the caval vein was occluded with another clip above its origin. The renal vein was punctured with a 26-gauge needle, and 0.3 ml of siRNA solution (NOX4 or XOR siRNA) was injected into the kidney. The two clips were removed immediately after the injection. The renal vein needle was held in place for 5–10 s after injection, then slowly removed, and the renal vein was gently compressed with a piece of Gelaspon (Chauvin Ankerpharm, Rudolstadt, Germany) for 30 s. Sham treatment was performed similarly with siNC non-sense sequences.

3.4. Pharmacologic Inhibitor Administration

Apocynin (APC; A10809, Sigma-Aldrich, Budapest, Hungary), an NADPH oxidase inhibitor, was administered intravenously (i.v.) 15 min before ischemia, then intraperitoneally (ip.) immediately at the start of reperfusion and 120 min after ischemia at a dose of 10 mg/kg body weight (BW). Oxypurinol (OXP; O6881, Sigma-Aldrich, Budapest, Hungary), a xanthine dehydrogenase inhibitor, was administered 30 minutes before (i.v.) and immediately after (i.p.) renal ischemia at a dose of 50 mg/kg BW. Equal volumes of the vehicle were injected as sham treatment.

3.5. Kidney Ischemia-Reperfusion

Mice were subjected to unilateral renal I/R with contralateral nephrectomy (Fig. 7), as previously described (88, 107, 108). In brief, the mice were anesthetized by i.p. injection containing a mixture of ketamine hydrochloride (80 mg/kg BW, CP-Pharma Handelsgesellschaft mbH, Germany) and xylazine (4 mg/kg BW, CP-Pharma Handelsgesellschaft mbH, Germany). During the operation, the core temperature of the body was maintained with the help of a heating pad (Supertech Ltd., Budapest, Hungary). Intraabdominal body temperature was monitored and registered during the ischemia procedure (36.7 ± 0.4ºC; mean ± SD). After median laparotomy, two occlusion clips were placed on the left renal pedicle to ensure secure occlusion for 10, 15, 20, or 30 min (Fig. 7). The right kidney was removed. The sham-operated mice underwent a similar operation, but the renal pedicle was not clamped. An additional group of non-operated (non-op) mice was sacrificed without prior surgery to evaluate the changes caused by invasive surgery in sham-operated mice.

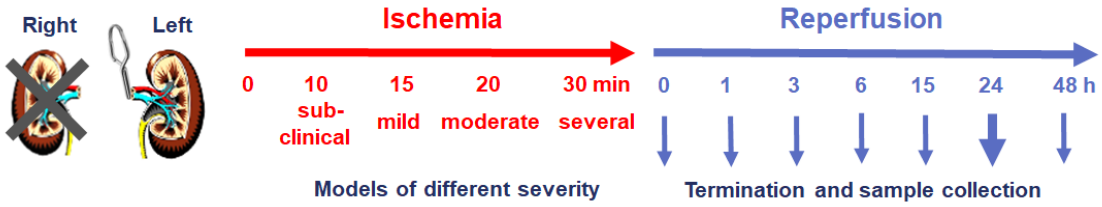

Figure 7. Study design of ischemia-reperfusion (I/R) surgery procedure. Ischemia operation was performed on the left kidney of the mice with contralateral nephrectomy. Changing the duration of the ischemia resulted in models of different severity. Reperfusion lasted different times, ending in termination and sample collection.

To prevent infections, Ceftriaxone (Rocephin, Roche Hungary Ltd., Budaörs, Hungary) was administered by subcutaneous (s.c.) injection at 20 mg/kg.

3.6. Animal Sacrifice and Sample Collection

The animals were sacrificed 1, 3, 6, 15, 24, or 48 hours after renal ischemia (Fig. 7). Mice received heparin i.p. (5000 U/kg BW, Ratiopharm GmbH, Ulm, Germany) and killed by cervical dislocation 3 min later. Blood was taken from the chest cavity after opening the chest and transecting the superior vena cava. The blood was centrifuged at 1500 g/10 min/4°C, and 100-µl plasma aliquots were pipetted into 500-µl Eppendorf tubes and stored at −80°C until use. The mice were placed in metabolic cages (Techniplast, Italy) for 24 hours for urine collection. The sediment was removed by centrifugation at 3000 g/20 min/4°C, and the urine samples were stored at -20°C. The blood was flushed from the circulation by left ventricular injection of 10 ml of cold (4 °C) physiological saline (Salsol A, Teva, Hungary). The kidney was cut into pieces, frozen in liquid nitrogen, and kept at −80 °C for morphological and molecular studies.

3.7. Plasma Urea/BUN Assay and Lipocalin-2/NGAL Immunoassay

The renal function was estimated by measuring the plasma urea concentration (Urea UV enzymatic, colorimetric kit, Diagnosticum Inc., Budapest, Hungary) as described by the manufacturer. Optical density was read at 340 nm using a Victor3™ 1420 Multilabel Counter (PerkinElmer, Wallac Oy, Turku, Finland). BUN values were calculated by dividing the urea concentrations by 2.14.

The concentration of plasma Lcn2 protein was assayed by ELISA (mouse Lipocalin-2/NGAL DuoSet ELISA Development kit; R&D Systems, Minneapolis, MI, USA). Briefly, 96-well plates (Nunc™ GmbH & Co. KG, Langenselbold, Germany) were coated with capture antibody, and non-specific binding sites were blocked with reagent diluent. Two parallel plasma samples were incubated for 2 hours, and then the detection antibody was added to all wells. Streptavidin-HRP was linked to the biotinylated detection antibody, followed by a short incubation with 3,3',5,5'-tetramethylbenzidine (TMB) substrate (Sigma-Aldrich Chemie GmbH, Steinheim, Germany). Before adding the substrate solution, the samples were washed with 300 µl wash buffer between each step (5 times). Optical density was read at 450 nm with wavelength correction set to 544 nm

(Victor3™ 1420 Multilabel Counter (PerkinElmer, Wallac Oy, Turku, Finland)). A four-parameter logistic curve fit was used to calculate the concentration of Lcn2 protein.

To distinguish between renal I/R damage and other causes of urinary Lcn2 elevation, we calculated the amount of filtered Lcn2. First, we estimated the glomerular filtration rate (GFR) based on BW, using previous observations on C57BL/6 mice, which reported a mean GFR of 951 ± 235 μL min^{-1} per 100 g BW. Then, we calculated the total volume filtered over the 24 hours and determined the amount of filtered Lcn2 using the following equation (107):

$$\text{Filtered Lcn2} = P_{[Lcn2]} \times Vol_{[24h\ GFR]},$$

where $P_{[Lcn2]}$ is the plasma Lcn2 concentration and $Vol_{[24h\ GFR]}$ is the 24-hour volume of the glomerular filtrate.

3.8. Renal Histology

Kidney tissue samples fixed in 4% buffered formaldehyde were dehydrated and embedded in paraffin wax (FFPE) for histological and immunohistochemical examination. Kidney morphology was evaluated microscopically on kidney sections stained with hematoxylin-eosin (HE) and periodic acid-Schiff (PAS).

Kidney sections were blindly scored. Acute tubular injury (ATI) was scored on a scale of 0 to 4 and calculated as the mean of 10 fields of view: 0 = normal histology; 1 = minimal or focal changes such as tubular cell swelling, mild brush border damage affecting less than 20% of the fields; 2 = more severe lesions, such as moderately dilated tubules, loss of brush border, presence of edematous tubular epithelial cells, weak focal nuclear staining covering approximately 25% of fields; 3 = extent of lesions, such as tubular injury, vacuolization of tubular epithelial cells, loss of brush border, loss of nuclear staining, covering 25-50% of fields; 4 = extension of the lesions, such as severe tubular necrosis, neutrophil granulocyte infiltration, loss of nuclear staining, dilated tubules, tubular cast formation in the lumen to more than 50% of the fields (108). To compare their sensitivities, tubular dilatation, cast, and necrosis were evaluated separately on kidney sections of different severity of renal ischemia (107).

Renal neutrophil infiltration and tubular epithelial cell injury were assessed using tissue microarray (TMA). The computer-controlled punch press of a TMA Master Device

(3DHISTECH Kft, Budapest, Hungary) cut 2 mm diameter cylinders in duplicate from each FFPE block for TMA. Myeloperoxidase (MPO) and Lcn2 immunohistochemistry (IHC) were also performed on TMA sections.

For MPO IHC (108), 4-μm thick sections were mounted on adhesive glass slides. The slides were boiled for 12 minutes in a mixture of 0.1 m Tris base and 0.01 m ethylenediaminetetraacetic acid (EDTA) (pH 9.0; Tris/EDTA) in an electric pressure cooker (AVAIR IDA, YDB50-90D; Biofa Ltd., Veszprém, Hungary) for heat-induced epitope retrieval (HIER). The plates were then incubated overnight with rabbit polyclonal anti-human MPO IgG (1:300, Agilent/Dako, Glostrup, Denmark), followed by a 30 min "post-primer block" and a 60 min incubation with peroxidase-labeled polymer using the Novolink polymer kit (RE7140-CE; Leica/NovoCastra, Newcastle upon Tyne, UK). The immune reactions were revealed in brown with the diaminobenzidine (DAB)-H_2O_2 chromogenic substrate system for 5-8 min under microscopic control. Finally, the slides were counterstained with hematoxylin and mounted on coverslips after dehydration.

Antigen retrieval for Lcn2 IHC (107) was performed by boiling the dewaxed and rehydrated TMA sections in a 0.01M Tris-HCl and 0.1 EDTA buffer (TBS; pH 9.0) for 25 min at 100°C. After incubating in 1% bovine serum albumin (BSA) in TBS (pH 7.4) for 15 min at room temperature, TMA sections were put in rabbit anti-human NGAL IgG (1:100; R&D Systems, Minneapolis, MI, USA) for 16 h, followed by goat anti-rabbit IgG EnVision-peroxidase polymer kit (Dako, Glostrup, Denmark) for 40 min. The tissue-bond peroxidase activity was developed with a DAB/H_2O_2 chromogen/substrate kit (Dako).

The immunostained TMA slides were digitized with a Pannoramic Scan instrument, and the staining was quantified by the Pannoramic Viewer v. 1.15 (3DHISTECH). MPO immunostaining was determined by the CellQuant module of the QuantCenter software v. 2.3 (3DHISTECH). Lcn2 staining intensity was quantified by ImageJ (NIH) software.

3.9. RNA Preparation

RNA samples extracted from the kidneys with TRI Reagent® (Molecular Research Center, Inc., Cincinnati, OH, USA) were kept at -80°C until use, as previously described (20). In brief, the frozen renal tissues were homogenized using an IKA® 1DI 18 basic ultra turrax (IKA Brasil Ltd, Taquora, Brazil). Chloroform (Sigma-Aldrich, Inc., Budapest, Hungary) was added to samples and mixed by vortexing. The aqueous phase

was separated by centrifugation. RNA was precipitated from the aqueous phase with an equal quantity of 2-propanol by incubation for 30 min at room temperature. The RNA pellet was washed twice with 75% ethanol and dissolved in 100 μl RNase-free water. DNase I (Fermentas, St. Leon-Rot, Germany) was used to eliminate DNA contamination, and the DNase was inactivated with phenol/chloroform extraction (Sigma-Aldrich, Inc., Budapest, Hungary). RNA concentration and purity were checked with a NanoDrop 2000c spectrophotometer (Thermo Fisher Scientific, Waltham, MA, USA). The absorbance ratio (260nm/280nm) was above 1.8 for all RNA samples. The samples were electrophoresed on 1% agarose gel (Invitrogen Ltd., Paisley, UK) in a BioRad Wide mini-sub1cell GT system (Bio-Rad Laboratories Inc., Hercules, CA, USA) to verify RNA integrity.

3.10. Quantitative PCR Analysis for mRNA Expression in Renal Tissue

Epidermal growth factor module-containing mucin-like hormone receptor-like 1 (EMR1 or F4/80), glutathione peroxidase 3 (GPX3), heme oxygenase 1 (HO-1), lipocalin-2 (Lcn2), NADPH oxygenase 2 (NOX2), NADPH oxygenase 4 (NOX4), nuclear factor erythroid 2–related factor 2 (NRF2), cytochrome b_{558} alpha subunit ($p22^{phox}$), tumor necrosis factor alpha (TNF-α) and xanthine oxidoreductase (XOR) mRNA expression was measured by double-stranded DNA (dsDNA) dye based real-time PCR. According to the manufacturer's protocol, reverse transcription into cDNA was performed using the High-Capacity cDNA Reverse Transcription Kit (Applied Biosystems, Foster City, CA, USA). In brief, 1 μg of total RNA was reverse transcribed into cDNA with random hexamer primers at 37°C for 2 hours in a BioRad iCycler™ Thermal Cycler (Bio-Rad Laboratories, Inc., Hercules, CA, USA). Using primer sequences of Integrated DNA Technologies (IDT, Table 1), the expression of mRNAs was quantified by a Bio-Rad C1000™ Thermal Cycler with CFX96™ Optics Module real-time PCR system (Bio-Rad Laboratories, Inc., Singapore). The primers were designed by NCBI/Primer-BLAST online, but we used the GPX3 primer sequence of Li et al. (109) and the NRF2 primer sequence of Hamada et al. (110). The qPCR reactions were performed with Maxima™ SYBR® Green qPCR Master Mix (Fermentas, St. Leon-Rot, Germany) and with SsoAdvanced™ Universal SYBR® Green Supermix (Bio-Rad Laboratories, Inc., Hercules, CA, USA), as described in the respective protocols. Primer

annealing was set to 58°C, and the melting curve was analyzed to detect any abnormality of the PCR product. All samples were measured in duplicates, and the expression of mRNAs was calculated using the relative quantification (ΔΔCq) method.

Table 1. Primers used for qPCR.

Target Gene	Forward Sequence (5' to 3')	Reverse Sequence (5' to 3')
18S	CTCAACACGGGAAACCTCAC	CGCTCCACCAACTAAGAACG
GAPDH	CCAGAATGAGGATCCCAGAA	ACCACCTGAAACATGCAACA
Lcn2	AGGTGGTACGTTGTGGGC	CTGTACCTGAGGATACCTGTG
NOX2	TGCCACCAGTCTGAAACTCAA	AGCAAAGTGATTGGCCTGAGA
NOX4	CCAGAATGAGGATCCCAGAA	ACCACCTGAACCATGCAACA
$p22^{phox}$	CGATCAGTGAGGACTTGCGA	CACACCTGCAGCGATAGAGT
XOR	GGCCATTTATGAAGCCTGTCA	GAAGTAGTGGAAGGGGTTCC
NRF2	CCTCACCTCTGCTGCAAGTA	GCTCATAGTCCTTCTGTCGCT
HO-1	ACAGAAGAGGCTAAGACCGC	GGCAGTATCTTGCACCAGG
TNF-α	AAATGGCCTCCCTCTCATCA	AGATAGCAAATCGGCTGACG
F4/80	TTTCCTCGCCTGCTTCTTC	CCCCGTCTCTGTATTCAACC
GPX3	CATCCTGCCTTCTGTCCCTG	CGATGGTGAGGGCTCCATAC

3.11. Statistical Analysis

Unless otherwise stated, all data are expressed as mean ± standard error of the mean (SEM). The homogeneity of group variances was checked using Bartlett's test. Depending on the results, one-way analysis of variance (ANOVA) with Dunnett's multiple comparison test or Kruskal-Wallis ANOVA by ranks and Dunn's test was used. A two-way ANOVA was used to evaluate the effects of ischemia and neutrophil deficiency. Two-way repeated measures ANOVA followed by Sidak's multiple comparisons test were used to compare the results of time-course experiments. The null hypothesis was rejected if $p<0.05$. Statistical analysis was performed using GraphPad Prism 8 (GraphPad Software Inc., San Diego, CA, USA).

DOI:10.14753/SE.2025.3164

4. RESULTS

4.1. Correlation Between the Duration of Ischemia and Renal Impairment

No histologic differences were found in the sections of the non-operated and the sham-operated kidneys (Fig. 8A-B, 8G-H, 8M-N, 8S-U). Blood urea nitrogen (BUN) did not increase after 10-minute renal ischemia compared to sham-operated animals (Fig. 8V).

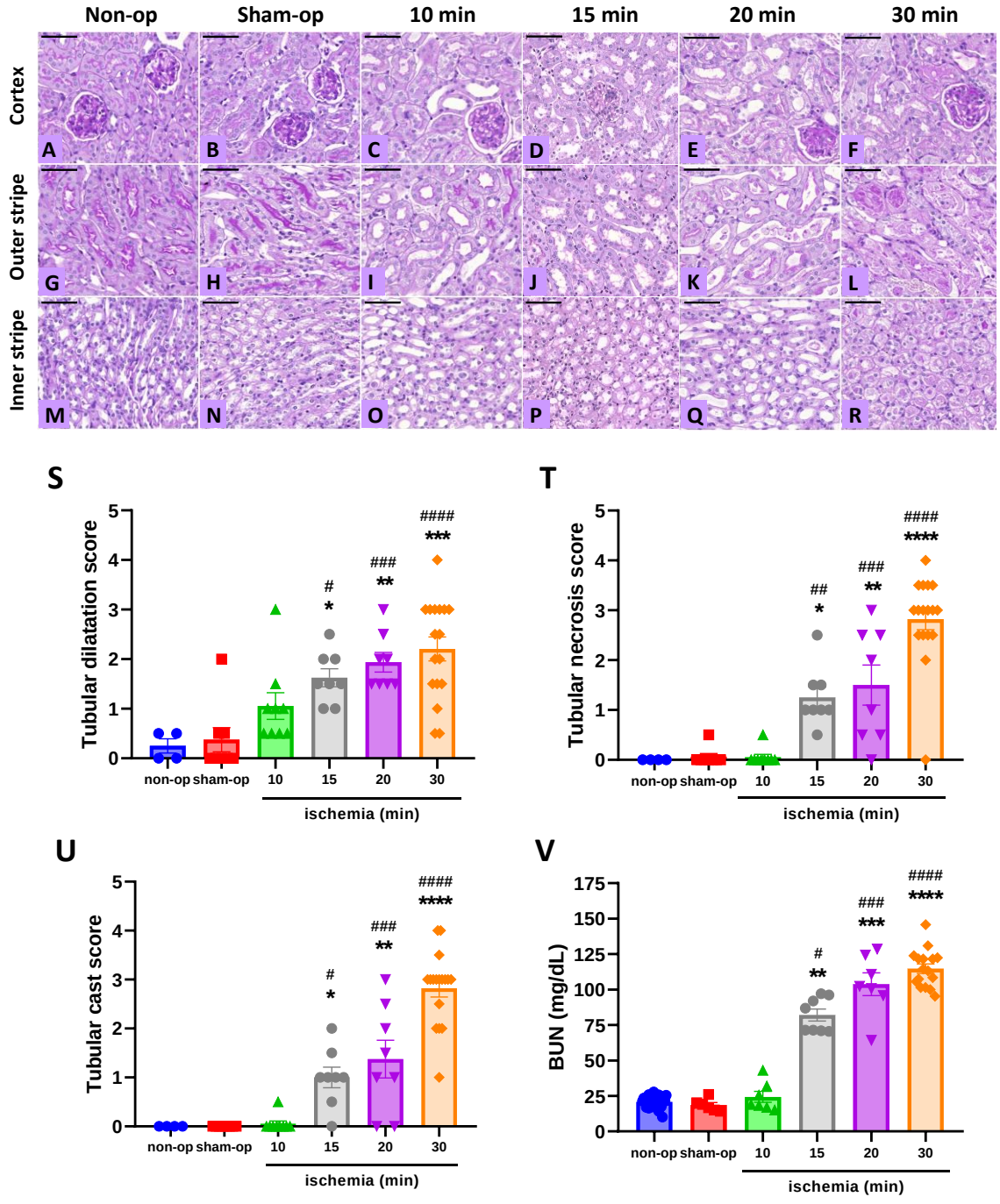

Figure 8. Histological findings of acute kidney injury (AKI) after different ischemic durations (107). The tubular dilation (S), tubular necrosis (T) and casts (U) scores and their histological manifestations in the kidney cortex, outer and inner stripes of the outer medulla after 10 minutes (C, I, O), 15 minutes (D, J, P), 20 minutes (E, K, Q) and 30 minutes (F, L, R) ischemia compared with the sham-operated (B, H, N) and non-operated (A, G, M) kidneys. Non-op/non-op: kidneys from animals without sham-operation (n = 4); Sham-op/sham-op: kidneys of sham-operated mice (n = 8); 10-min/10: 10-minute renal ischemia (n = 9); 15-min/15: 15-minute renal ischemia (n=8); 20 min/20: 20-minute renal ischemia (n = 8); 30 min/30: 30-minute renal ischemia (n = 17). (V) Blood urea nitrogen (BUN) as a marker of glomerular filtration rate (GFR). One-way ANOVA with Dunnett's post hoc test; non-op: n = 34; ctrl-op: n = 6; 10-min: n = 7; 15-min: n=8; 20-min: n = 7; 30-min: n = 16; *p<0.05, **p<0.01, ***p<0.001, ****p<0.0001 vs. non-op; $^{\#}$p<0.05, $^{\#\#}$p<0.01, $^{\#\#\#}$p<0.001, $^{\#\#\#\#}$p<0.0001 vs. sham-op.

Only minor changes in the morphology were found in the histological sections of the 10-minute group, i.e., the tubular dilation score was higher in the 10-minute group than in the sham (Fig. 8S). The tubular dilation score (Fig. 8S) was the most sensitive parameter, which already showed an increasing trend after 10-minute ischemia and significantly increased after 15-minute ischemia compared to the sham-operated kidneys. Otherwise, the kidneys had normal histology in the 10-minute renal ischemia group (Fig. 8C, I, O, and 8S-U).

The first clear morphological signs of ischemia-reperfusion (I/R) injury (IRI) were detected after the 15-minute renal ischemia (8D, J, and P), which was quantified by elevated scores (Fig. 8S-U). An increase in renal urea retention also indicated renal functional impairment (Fig. 8V) at the exact duration of ischemia. Acute kidney injury (AKI) due to 15-minute ischemia was classified as mild IRI based on mild histological injury and functional impairment.

Renal injury after the 20-minute ischemia was classified as moderate IRI as more significant increases in tubular dilatation, necrosis, and cast scores were apparent (Fig. 8E, K, Q, and 8S-U). The histological damage was also functionally reflected in the much higher plasma BUN in the 20-minute renal I/R group compared to the sham-operated group (Fig. 4V).

Thirty minutes of renal ischemia, defined as severe IRI, caused extensive tubule dilatation and necrosis, as well as cast accumulation in the renal cortex and medulla (Fig.

8F, L, and 8R-U) with a significant increase in plasma BUN compared with sham-operated animals (Fig. 8V).

The tubular dilation score (Fig. 8S) was the most sensitive parameter, which already showed an increasing trend after 10 minutes of ischemia (Fig. 8C, I, O) and significantly increased after 15 minutes of ischemia (Fig. 8D, J, P) compared to the sham-operated (Fig. 8B, H, N) kidneys. Tubular necrosis and casts were first present after 15 minutes of ischemia (Fig. 8D, J, P) and proportionally increased after 20 (Fig. 8E, K, Q) and 30 minutes (Fig. 8F, L, R) of ischemia. No significant histologic change existed between non-operated (Fig. 8A, F, and K) and sham-operated (Fig. 8B, H, and N) kidneys. Compared to the non-op, the sham operation and 10-minute ischemia did not affect the kidney function by blood urea nitrogen (BUN). BUN retention increased with the duration of ischemia, indicating a proportional aggravation of the renal impairment (Fig. 8V).

4.2. Time Course of Kidney Impairment and Morphological Damage Due to Ischemia-Reperfusion

BUN, plasma lipocalin-2 (Lcn2) concentrations, renal Lcn2 mRNA expression, and acute tubular injury (ATI) scores in our time course study were similar to those in the sham-operated mice and animals after 30 min of renal ischemia in our laboratory (88, 107, 108) (Fig. 9A-C and 8V). BUN concentration gradually increased from 19.2 ± 2.0 mg/dL to 77.9 ± 4.5 mg/dL at 6 h and 286.7 ± 29.8 mg/dL at 48 h (Fig. 9A) after 30 min ischemia. The plasma concentration (Fig. 9B) and renal mRNA of Lcn2 (Fig. 9C) reached a 10-fold and 100-fold plateau by 15 h compared to the sham-operated group.

The mRNA expression of oxidase enzymes xanthine oxidoreductase (XOR) and NADPH oxidases (NOX) was low in sham-operated kidneys. After the sham operation, XOR mRNA increased 2.3-fold after 6 hours (Fig. 9D). In contrast, compared with the sham-operated kidneys, XOR mRNA levels began to increase 15 h after ischemia, increased 5-fold at 24 h and remained elevated at 48 h after severe (30 min) ischemia (Fig. 9D). Meanwhile, the expression of NADPH oxidases peaked at 1-3 hours, gradually recovered at 15 hours after ischemia, but remained elevated at 24 or 48 hours (Fig. 9E). Additionally, a small second peak in NOX2 gene expression was observed at 24 h when neutrophil infiltration peaked (Fig. 9E). The expression of NOX2, NOX4, and $p22^{phox}$

DOI:10.14753/SE.2025.3164

mRNA reached a maximum increase of six-fold, four-fold, and three-fold, respectively, 3 hours after reperfusion (Fig. 9E).

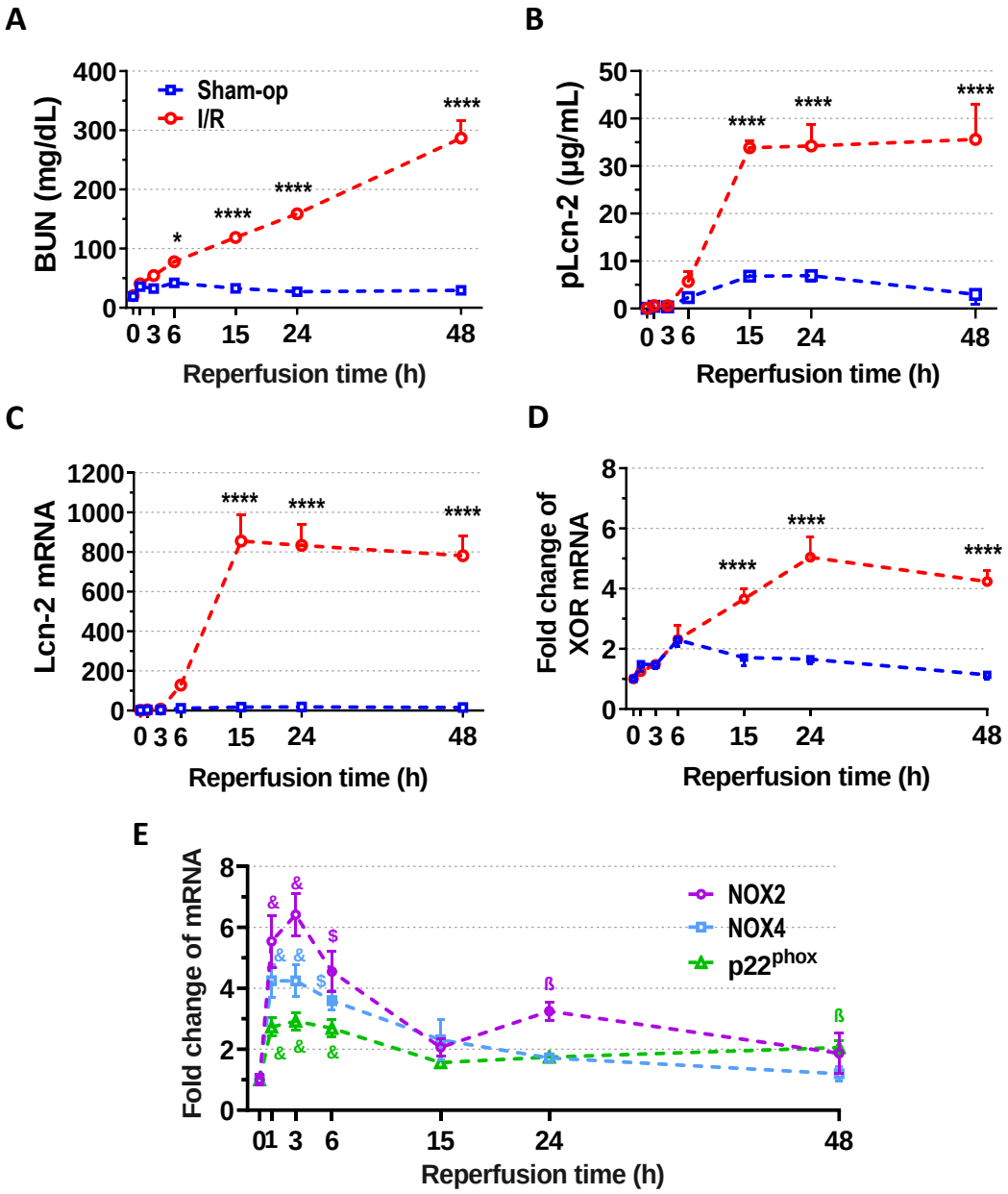

Figure 9. Postischemic time course of kidney function and oxidase enzyme mRNA expression after 30-min ischemia (108). (A) Blood urea nitrogen (BUN), (B) lipocalin-2 (Lcn2) plasma concentration, (C) renal Lcn2 gene expression, and mRNA expression of (D) xanthine oxidoreductase (XOR) and (E) NADPH oxidases (NOX2, NOX4, $p22^{phox}$). Sham-op: sham-operated group. I/R: ischemia-reperfusion group. (A-D) *p<0.05, ****p<0.0001 vs sham-op. (E) $^{ß}p<0.05$, $^{\$}p<0.001$, $^{\&}p<0.0001$ vs 0-hour group. Two-way ANOVA with Sidak post hoc test. n=5/group/time.

Functional impairment assessed by BUN indicates a continuous, ongoing injury with an early start when NOX, not XOR, is upregulated (Fig. 9A, D, and E). The robust increase in the expression and blood level of the injury marker Lcn2 outruns the XOR upregulation (Fig. 9B, C, and D).

Morphological evidence of ATI appeared starting at 3 h after ischemia, and the ATI score reached a maximum of 3 at 24 and 48 h after reperfusion (Fig. 10A and C). Immunohistochemistry for MPO showed continuous neutrophil infiltration in the inner medulla and inner stripe of the outer medulla as early as 3 hours after 30 min of ischemia (Fig. 10B-C). Neutrophils began to appear in the cortex and the outer stripe of the outer medulla after 6 hours, and their presence around the injured tubules was particularly noticeable at 15 hours after ischemia (Fig. 10C). After reaching the peak at 24 hours, a slight decrease in infiltration was observed at 48 hours. At 24 hours after ischemia, dilated tubules with flattened epithelial cells were the primary morphological markers of postischemic kidney injury (Fig. 10C). The most intense infiltration was detected in the outer stripe of the outer medulla, with the highest number of MPO-positive cells occurring at 24 h and neutrophils still present around the necrotic tubules at 48 h.

DOI:10.14753/SE.2025.3164

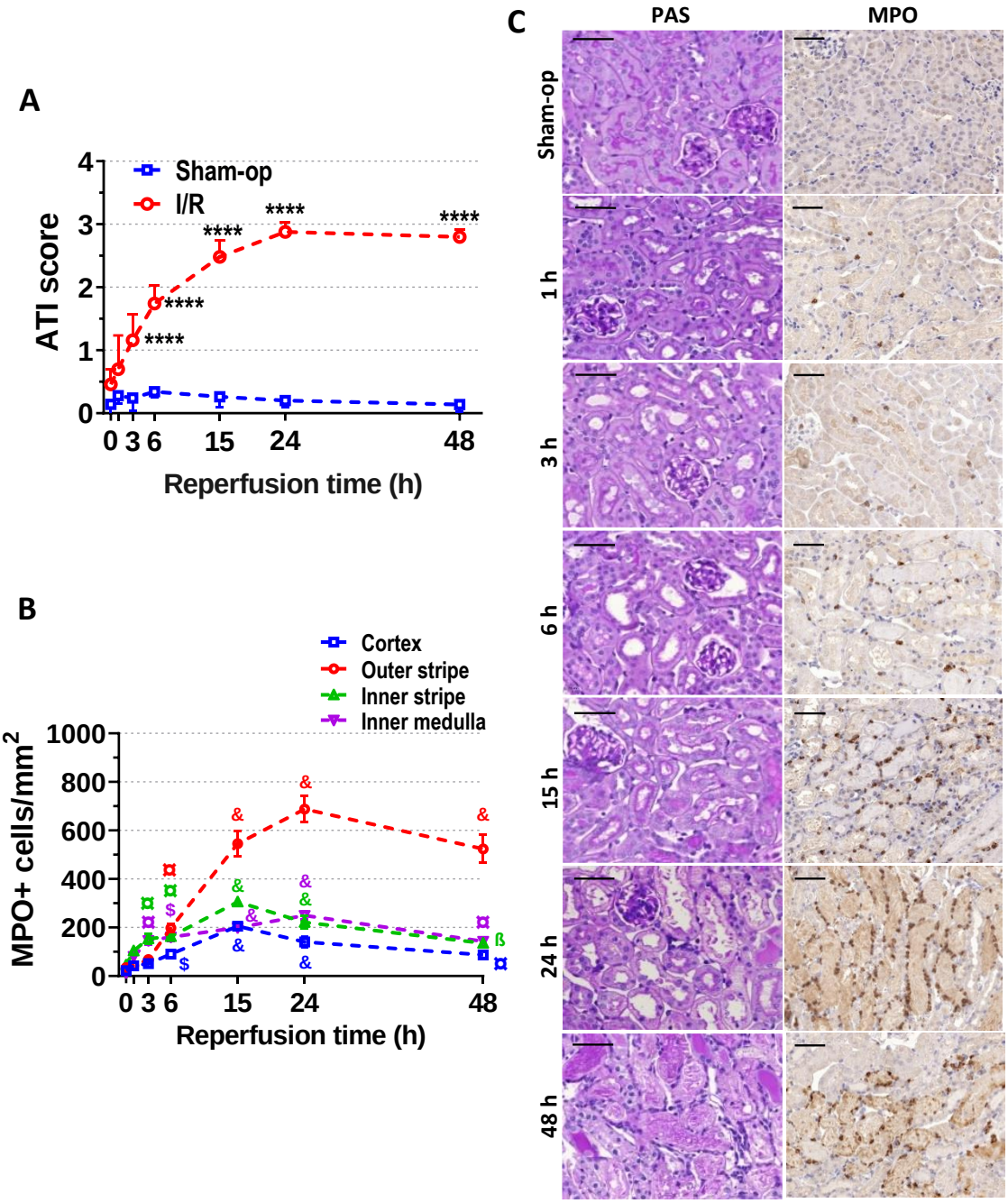

Figure 10. Postischemic time course of kidney morphology and neutrophil infiltration after 30-min ischemia (108). (A) Acute tubular injury (ATI) score, (B) MPO+ cell count, (C) periodic acid-Schiff (PAS) staining, and myeloperoxidase (MPO) immunohistochemistry. Scale bar: 50 µm. Sham-op: sham-operated group. I/R: ischemia-reperfusion group. (A) ****p<0.0001 vs sham-op. (B) ßp<0.05, ¤p<0.01, $p<0.001, &p<0.0001 vs 0-hour group. Two-way ANOVA with Sidak post hoc test. n=5/group/time.

DOI:10.14753/SE.2025.3164

4.3. Pharmacological Inhibition of NADPH Oxidase Enzymes but Not Xanthine Oxidoreductase Protected against Mild but Not Moderate or Severe Renal Ischemia

Compared to the sham-operated animals, renal ischemia of various durations increased all renal injury markers (BUN and Lcn2 concentrations, Lcn2 renal gene expression, and ATI score) in proportion to the severity of ischemia (Fig. 11A-E).

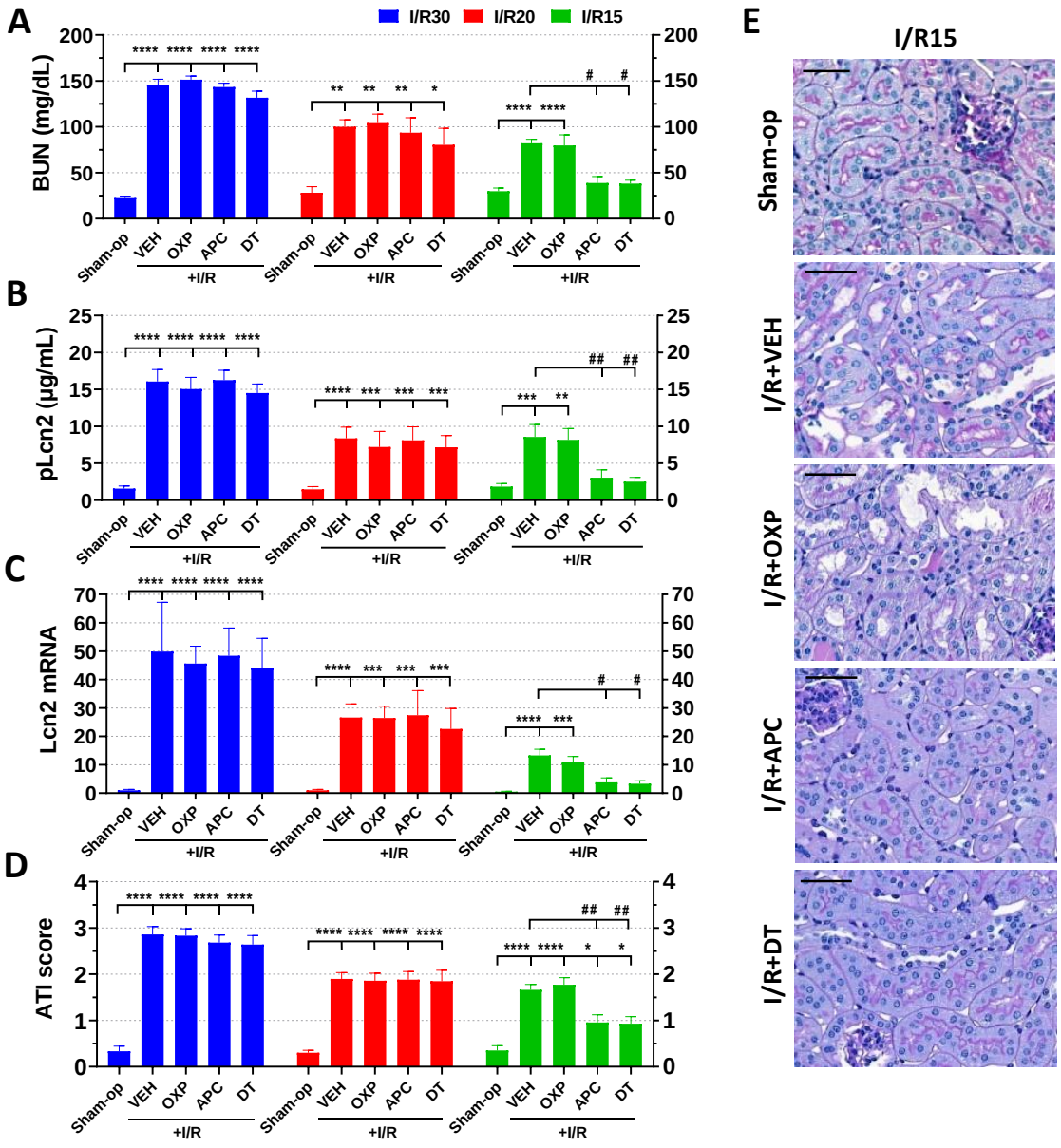

Figure 11. NADPH oxidase inhibition by apocynin attenuated functional and morphological damage depending on the severity of ischemia, while inhibition of xanthine oxidase activity by oxypurinol was ineffective (108). (A) BUN, (B) Lcn2 plasma concentration, (C) renal Lcn2 gene expression, (D) ATI score, (E) renal histology (periodic acid-Schiff (PAS) staining; scale bar: 50

μm), Sham-op: sham-operated group. I/R: ischemia-reperfusion group. I/R15, 20, 30 refers to the duration of ischemia (min). VEH: vehicle treatment, APC: apocynin, OXP: oxypurinol, DT: double treatment. *p<0.05, **p<0.01, ***p<0.001, ****p<0.0001 vs sham-op. #p<0.05, ##p<0.01 vs IR+VEH. One-way ANOVA with Dunnett's post hoc test; I/R30: n=6-5-7-7-6; I/R20: n=5-7-7-6-6; I/R15: n=6-8-7-7-7.

Apocynin, a pan-NOX inhibitor, improved renal function and morphology at 24 h after mild (15 min) but not moderate (20 min) or severe (30 min) ischemia (Fig. 11A-E). Oxypurinol, an XOR inhibitor, did not improve renal function and morphology after renal ischemia of either severity (Fig. 11A-E). Furthermore, a combination of the two inhibitors, apocynin and oxypurinol, was similarly effective as apocynin alone (Fig. 11A-E).

4.4. Pharmacological Inhibition of NADPH Oxidases by Apocynin Increased Antioxidant Defense and Attenuated Inflammation after Mild Renal Ischemia

Apocynin mitigated functional impairment and morphological damage when the kidneys were subjected to mild (15 min) I/R (Fig. 12A-E). Furthermore, combined treatment with apocynin and oxypurinol was as effective as apocynin alone, indicating that inhibition of XOR had no additive effect (Fig. 12A-E). The protective impact of apocynin was confirmed in gene expression related to inflammation and antioxidant activity. Mild renal I/R increased mRNA expression of tumor necrosis factor alpha (TNF-α) by 15-fold, F4/80 by 60-fold, and heme oxigenase 1 (HO-1) by 7-fold, while glutathione peroxidase 3 (GPX3) decreased to 50% of control values and had no effect on nuclear factor erythroid 2-related factor 2 (NRF2) mRNA expression at 24 h post-ischemia, compared to the sham-operated group (Fig. 12A-E).

Apocynin administration increased renal NRF2 expression by 2.8-fold and I/R-induced HO-1 expression from 7-fold to 44-fold in the postischemic kidneys of mice subjected to mild I/R compared with the vehicle-treated group (Fig. 12C-D). In addition, apocynin lowered the TNF-α and F4/80 mRNA expression (Fig. 12A-B) and prevented the reduction of GPX3 gene expression in the kidney (Fig. 12E).

DOI:10.14753/SE.2025.3164

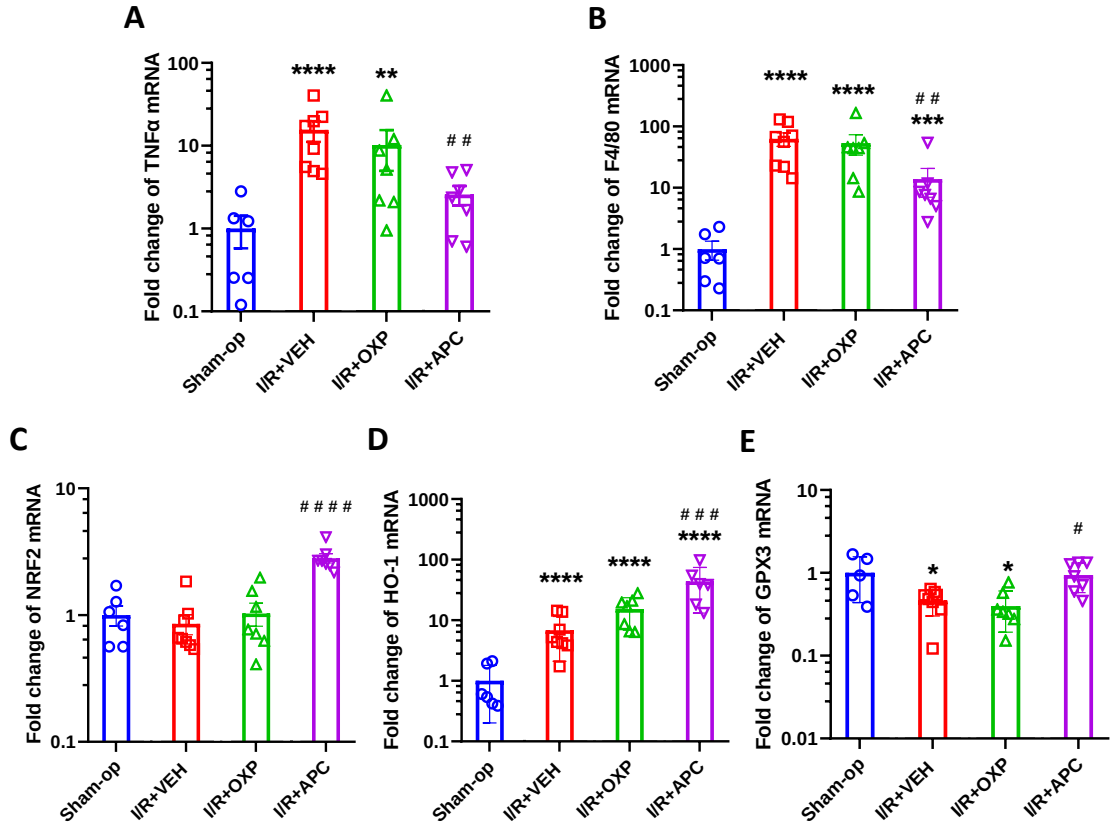

Figure 12. The effects of apocynin on the mRNA expression of (A) TNFα, (B) F4/80, (C) NRF2, (D) HO-1, (E) GPX3 after mild (15 min) renal ischemia. VEH: vehicle, APC: apocynin, OXP: oxypurinol, *p<0.05, **p<0.01, ***p<0.001, ****p<0.0001 vs. sham-op. #p<0.05, ##p<0.01, ###p<0.001, ####p<0.0001 vs. I/R + VEH. One-way ANOVA with Dunnett's post hoc test; sham n = 6, I/R + VEH n = 8, I/R + inhibitor groups n = 7 (108).

4.5. Xanthine Oxidoreductase and NAPDH Oxidase 4 Silencing Did Not Protect Renal Function after Ischemia

Renal I/R significantly increased all the kidney injury markers (BUN, Lcn2 concentrations, and Lcn2 mRNA) and morphologic damage (ATI score) at 24 hours after severe (30 min) and mild (15 min) ischemia (Fig. 13A-E). Despite the effective silencing of XOR and NOX4, no improvement in renal function was observed after either severe (30 min) or mild (15 min) renal ischemia (Fig. 13A-E). Histological sections of the siRNA-silenced groups showed renal morphological damage similar to non-coding siRNA-treated I/R animals (Fig. 13D-E), confirming that knockdown of the targeted oxidative enzymes has no therapeutic effect against renal IRI.

DOI:10.14753/SE.2025.3164

XOR mRNA expression increased more than 5-fold and 3-fold 24 h after severe (30 min) or mild (15 min) renal ischemia, respectively (Fig. 13F). XOR siRNA fully (15 min) or partially (30 min) reversed the ischemia-induced increase in XOR mRNA expression with 66% knockdown efficiency in both cases (Fig. 13F).

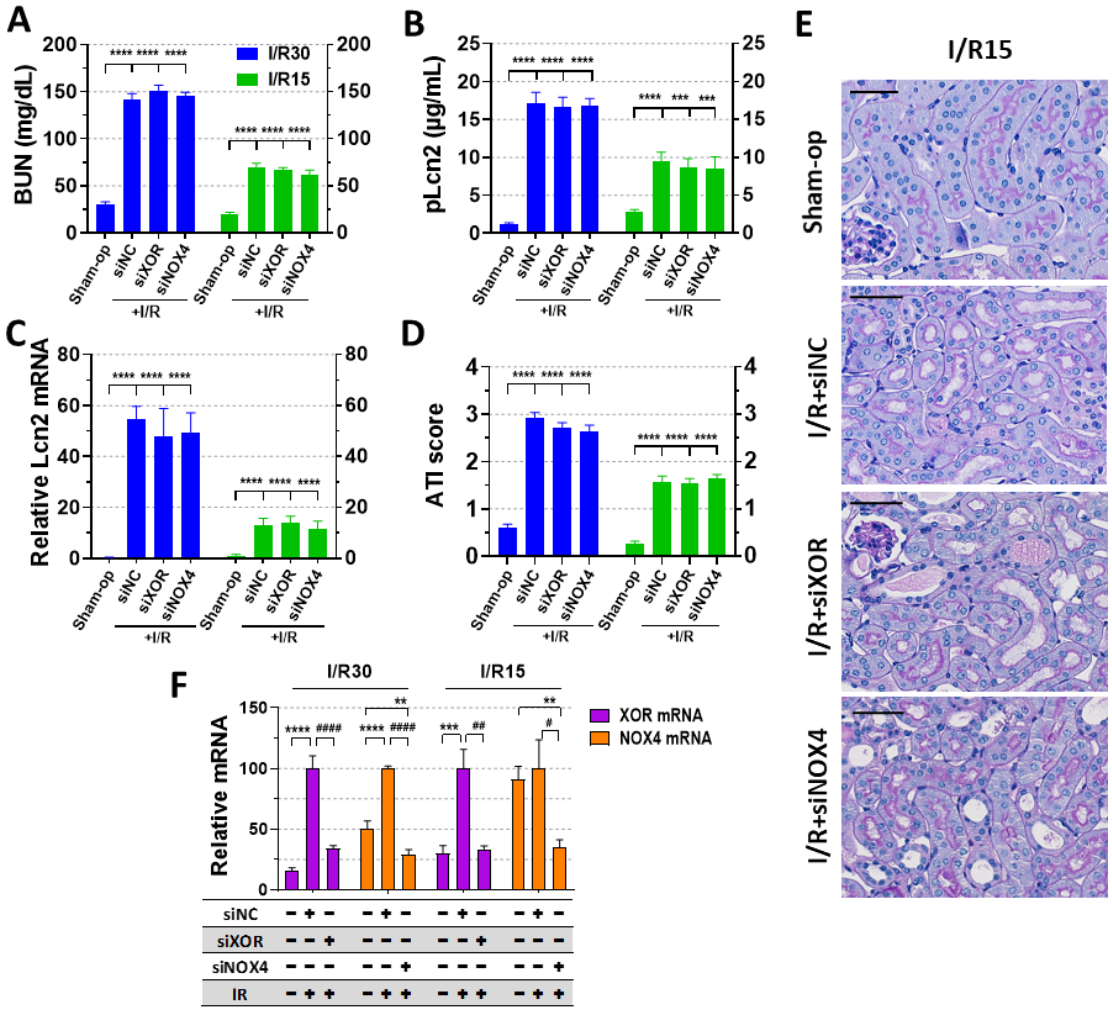

Figure 13. Kidney function and morphology after siRNA-mediated knockdown of XOR and NOX4 genes (108). (A) BUN, (B) Lcn2 plasma concentration, (C) renal Lcn2 gene expression, (D) ATI score, (E) renal histology (periodic acid-Schiff (PAS) staining; scale bar: 50 µm), (F) RNAi silencing efficiency. Sham-op: sham-operated group. I/R: ischemia-reperfusion group. siNC: treatment with non-coding siRNA. I/R15 and I/R30 refer to the duration of ischemia (min). **p<0.01, ***p<0.001, ****p<0.0001 vs Sham-op. #p<0.05, ##p<0.01, ####p<0.0001 vs IR+VEH. One-way ANOVA with Dunnett's post hoc test; I/R30: n=7-8-9-9; I/R15: n=8-8-8-7.

Renal NOX4 expression approx. doubled at 24 hours after 30 min ischemia but remained unchanged at 24 hours after 15 min ischemia (Fig. 13F). RNAi using NOX4 siRNA inhibited the ischemia-induced increase in NOX4 mRNA. SiRNA-based knockdown reduced NOX4 mRNA below the control level with 71% silencing efficiency in the 30-min I/R study, while knockdown efficiency was 65% in the 15-min I/R experiment.

4.6. Neutrophil-Deficient Mice Are Protected from Mild Renal Ischemia-Reperfusion Injury

Neutrophil granulocytes were virtually absent from the circulation of conditional Mcl-1-deficient bone marrow-transplanted (Mcl-$1^{\Delta Myelo}$) chimeric mice. The proportion of neutrophils increased in the blood of wild-type (WT) mice at 24 hours after I/R (Fig. 14C and 14N).

Following 20 min of ischemia, a marked increase in BUN and Lcn2 concentrations was observed in WT compared to sham-operated animals (Fig. 14A-B). The neutrophil-deficient Mcl-$1^{\Delta Myelo}$ mice showed milder but significant increases in BUN and Lcn2 concentrations after 20 min of ischemia (Fig. 14A-B). In contrast, changes in BUN and Lcn2 concentrations, renal Lcn2 mRNA expression, and ATI score were significantly lower in neutrophil-deficient than in WT mice after mild, 15-min renal ischemia (Fig. 14D-G). Histological sections revealed preserved morphology in the kidneys of the neutrophil functional knockout mice compared to WT animals (Fig. 14H). TNF-α, F4/80, and HO-1 expression increased, GPX3 decreased, and NRF2 did not change in WT mice 24 hours after mild ischemia (Fig. 14I-M). In contrast, none of these mRNAs were altered in the kidneys of neutrophil-deficient mice (Fig. 14I-M). The histological damage in the kidneys of Mcl-$1^{\Delta Myelo}$ mice was also alleviated (Fig. 14H).

DOI:10.14753/SE.2025.3164

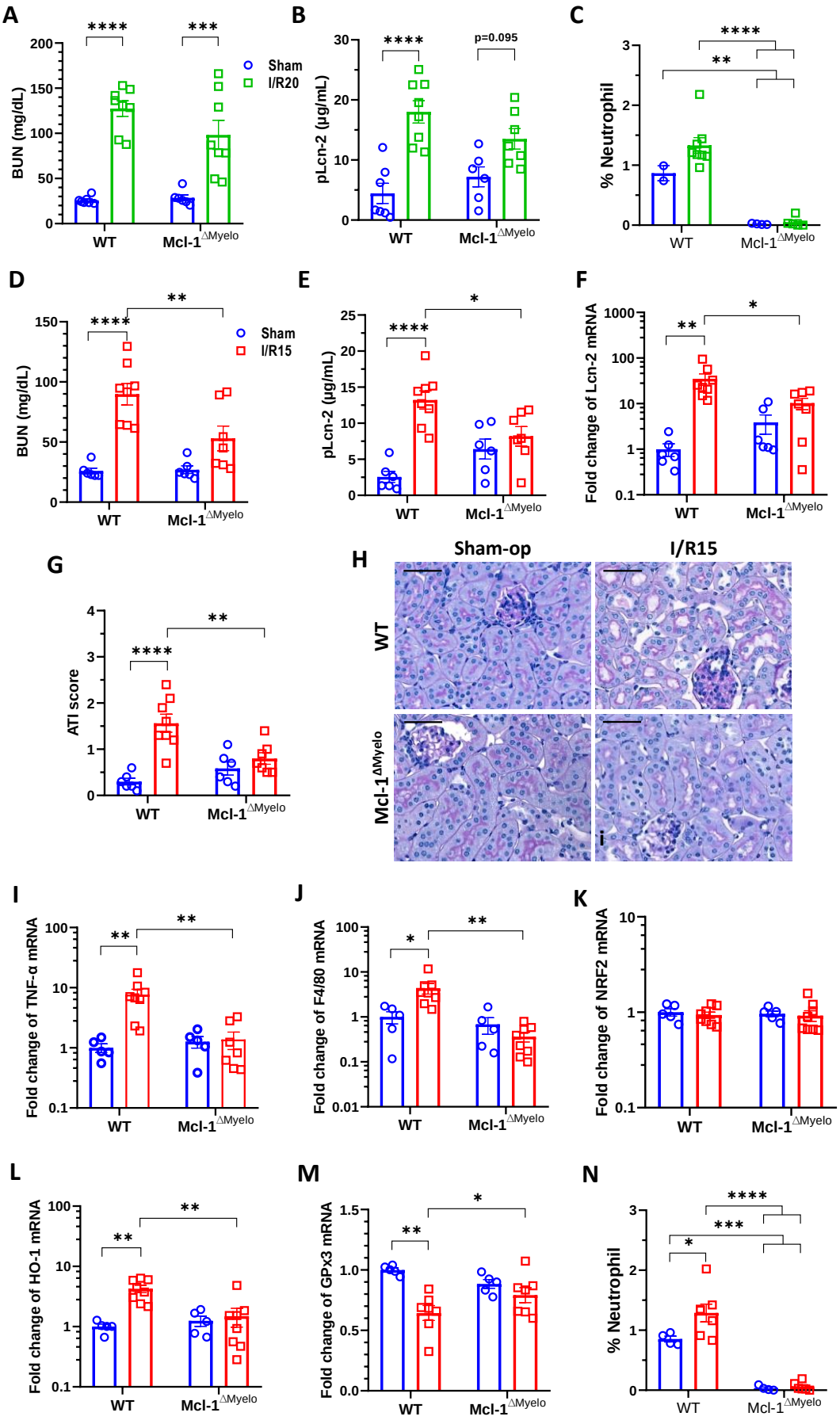

Figure 14. Kidney function and histology in neutrophil-deficient bone marrow chimeric mice after moderate (20 min) and mild (15 min) renal ischemia-reperfusion injury (IRI) (108). (A) BUN, (B) Lcn2 plasma concentration, (C) the proportion of neutrophils in the blood after moderate (20 min) renal ischemia. (D) BUN, (E) plasma Lcn2 concentration, (F) renal Lcn2 gene expression, (G) ATI score, (H) renal histology (periodic acid-Schiff (PAS) staining; scale bar: 50 μm), (I) TNFα, (J) F4/80, (K) NRF2, (L) HO-1, (M) GPX3 mRNA expression, (N) the proportion of neutrophils in the circulation after mild (15 min) renal ischemia. Sham-op: sham-operated group. I/R: ischemia-reperfusion group. WT: wild type, Mcl-$1^{\Delta Myelo}$: neutrophil-deficient bone marrow chimeric mice. *p<0.05, **p<0.01, ***p<0.001, ****p<0.0001. Two-way ANOVA with Tukey's post hoc test. (A-B) Kidney function/injury: WT sham n=6; Mcl-$1^{\Delta Myelo}$ sham n=7; I/R groups n=8 (C) FACS: WT sham n=2; WT Mcl-$1^{\Delta Myelo}$ n=4; WT I/R n=8; Mcl-$1^{\Delta Myelo}$ I/R n=5 (D-G) Renal function/histology: sham groups n=6; WT I/R n=8; Mcl-$1^{\Delta Myelo}$ I/R n=7; (I-M) mRNA expression: sham n=5; I/R n=8; (N) FACS: sham groups n=4; WT I/R n=7; Mcl-$1^{\Delta Myelo}$ I/R n=6.

4.7. Lipocalin-2 Induction after Kidney Ischemia-Reperfusion

A mild, diffuse cytoplasmic Lcn2 staining was observed only in the renal cortex but not in the renal medulla of unoperated mice. (Fig. 15A, F, and K). The area and intensity of cortical Lcn2 staining were more extensive, and Lcn2 also appeared in the renal medulla of sham-operated mice. (Fig. 15B, G, and L). Ischemia-reperfusion injury increased Lcn2 staining mainly in the medulla (Fig. 15H–J and 15M–O). Interestingly, the area and intensity of cortical Lcn2 staining increased markedly and similarly in all mice subjected to surgery with or without ischemia-reperfusion (Fig. 15B–E and 15T).

On the other hand, increasing ischemia times were associated with gradually rising Lcn2 staining in the outer (Fig. 15U) and the inner stripe of the medulla (Fig. 15V). Thus, ischemia time alone affected only medullary, not cortical, Lcn2 staining. In the tubular epithelial cells of the proximal tubules, characteristic punctate Lcn2 staining pattern (Fig. 15P-R) was present in non- and sham-operated mice (Fig. 15P and Q), but it was more intense after severe (30 min) ischemia (Fig. 5R). Tubular casts and necrotic tubules were also Lcn2 positive (Fig. 15J and O) after severe ischemia. No Lcn2 staining was detected without the primary antibody (Fig. 15S).

DOI:10.14753/SE.2025.3164

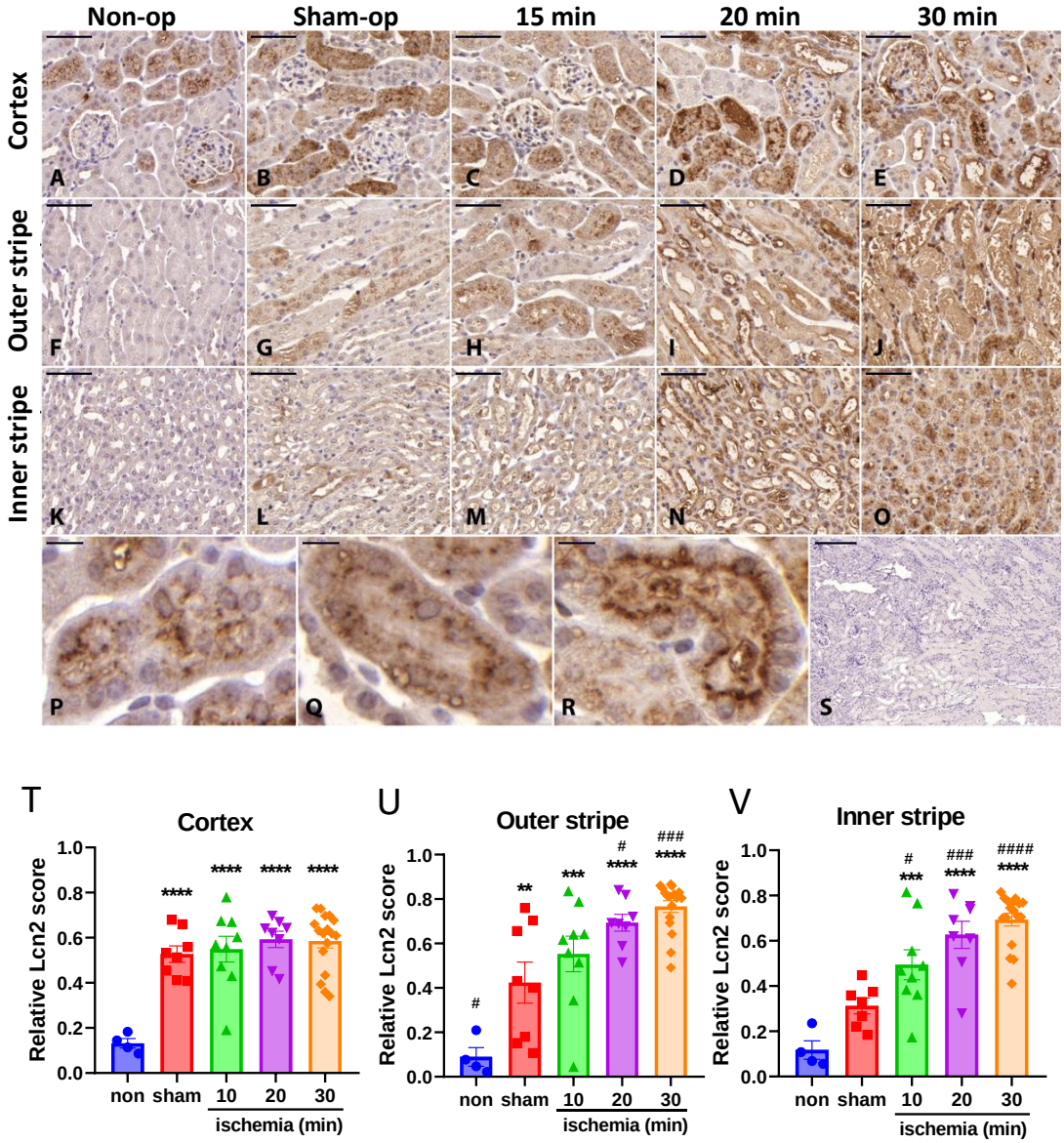

Figure 15. The intensity and extent of lipocalin-2 (Lcn2) immunostaining (A-E) in the cortex, (F-J) outer stripe, and (K-O) inner stripe of the medulla in the kidneys of non-operated (A, F, and K) and sham-operated mice (B, G, L), and of mice subjected to 10-min (C, H, M), 20-min (D, I, N) 30-min (E, J, O) renal ischemia-reperfusion (I/R) injury (107). High-magnification images of the intracellular staining pattern of Lcn2 in the kidneys of non-operated (P), sham-operated (Q), and I/R (R) mice. (S) Lcn2 staining without the primary antibody. Scale bar: (A-O) 50 µm, (P-R) 10 µm, (S) 200 µm; non-op/non: kidneys of non-operated mice; sham-op/sham: kidneys of sham-operated mice; 10 min/10: 10-minute renal ischemia; 20 min/20: 20-minute renal ischemia; 30 min/30: 30-minute renal ischemia. **p<0.01, ***p<0.001, ***p<0.0001 vs. non-op; $^{\#}$p<0.05, $^{\#\#\#}$p<0.001, $^{\#\#\#\#}$p<0.0001 vs. sham-op; non-op: n = 4; sham-op: n = 8; 10 min: n = 9; 20 min: n = 8; 30 min: n = 17.

DOI:10.14753/SE.2025.3164

4.8. Plasma Concentration, Urinary Excretion, and Renal Expression of Lipocalin-2 Are Markers of Renal Ischemia-Reperfusion Injury

Normalization of urinary lipocalin-2 (uLcn2) excretion to urinary creatinine (uCr) gave similar results to that of 24-hour uLcn2 excretion (Fig. 16A). Plasma Lcn2 concentration, renal Lcn2 mRNA expression, and urinary Lcn2 excretion significantly increased after sham surgery (Fig. 16B-D) compared with no surgery. Surprisingly, renal Lcn2 mRNA expression and plasma Lcn2 concentration similarly increased after 10 min of renal ischemia and sham operation (Fig. 16B-C). However, urinary Lcn2 excretion increased much more after 10 min of renal ischemia than after a sham operation (Fig. 16D).

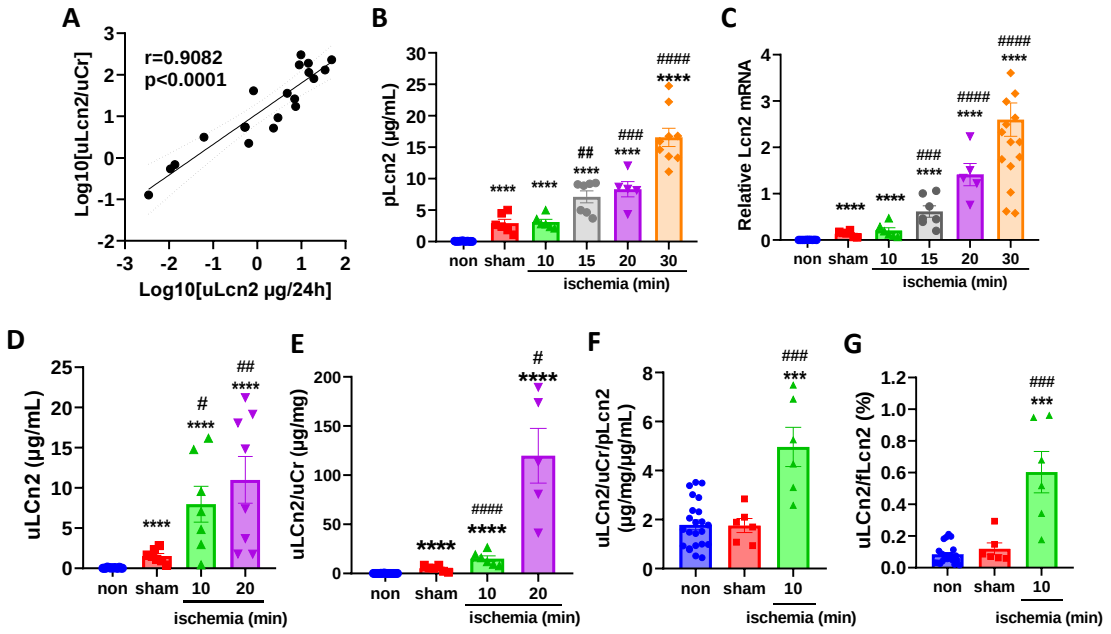

Figure 16. Lipocalin-2 (Lcn2) biomarker to detect ischemia-reperfusion injury (IRI) (107). (A) Urinary Lcn2 (uLcn2) normalized to urinary creatinine (uCr) correlated significantly with 24-hour uLcn2. (B) Plasma concentration, (C) renal mRNA expression, and (D) urinary Lcn2 (uLcn2) concentration. (E) Urinary Lcn2 excretion normalized to excreted urinary creatinine (uCr), (F) Urinary Lcn2 further normalized to plasma Lcn2 (pLcn2). (G) The ratio between uLcn2 and calculated filtered Lcn2 (fLcn2). non: non-operated mice; sham: sham-operated mice; 10: 10-minute renal ischemia; 15: 15-minute renal ischemia; 20: 20-minute renal ischemia; 30: 30-minute renal ischemia. One-way ANOVA with Dunnett's post hoc test. *p<0.05, ***p<0.001 ****p<0.0001 vs. non-op; #p<0.05, ##p<0.01, ###p<0.001, ####p<0.0001 vs. sham; non: urine and plasma n = 23, kidney RNA n = 10; sham: n = 6; 10 min: n = 6; 20 min: n = 5; 30 min: plasma and kidney RNA n = 17.

Thus, only urinary Lcn2 excretion distinguished 10-min renal ischemia from sham operation. Twenty- to thirty-minute renal ischemia resulted in massive elevations of renal Lcn2 mRNA expression and plasma Lcn2 concentration (Fig. 16B-C). Urinary Lcn2 excretion was much higher after 10 min of ischemia than after a sham operation, such as the uLcn2 after 20 min of ischemia than after 10 min of ischemia (Fig. 16D-E). The aggravation of renal injury indicated by Lcn2 correlated with the duration of ischemia (Fig. 16B-E).

We calculated the ratio of urinary Lcn2 (uLcn2) excretion to plasma Lcn2 (pLcn2) levels. Importantly, u/pLcn2 values were similar in the sham-operated and non-operated groups (Fig. 16F). However, the u/pLcn2 ratio significantly increased after 10-min ischemia compared to the sham-operated mice and was further elevated after more severe ischemia (Fig. 16F). To better understand the difference in urinary Lcn2 excretion after 10-minute ischemia and sham operation, we compared the excreted uLcn2 to the estimated filtered Lcn2 (fLcn2) in both groups. The excreted uLcn2 was about 6-fold higher than the fLcn2 after 10-min ischemia. However, they were similar after sham and no operation (Fig. 6G), suggesting that the postischemic kidney added a large amount of Lcn2 to the excreted fraction.

The diagnostic value of u/pLcn2 compared to other kidney injury markers was further evaluated using Receiver Operating Characteristics (ROC) curve analysis (Tables 2 and 3).

Table 2. The ability of plasma and urinary Lcn2 and BUN levels to discriminate between the severity of renal ischemia-reperfusion injury compared to sham operation (107).

Ischemia vs. sham-op	**10 min**				**20 min**			
Kidney damage marker	**Area**	**SE**	**P**	**Cut-off**	**Area**	**SE**	**P**	**Cut-off**
BUN (mg/dL)	0.60	0.16	0.52	N/A	1.00	0.00	**0.01**	46.920
Lcn2 mRNA	0.67	0.16	0.32	N/A	1.00	0.00	**0.01**	0.410
pLcn2 (µg/mL)	0.58	0.18	0.63	N/A	0.93	0.08	**0.05**	3.498
uLcn2 (µg/24h)	0.86	0.14	**0.01**	2.385	0.90	0.10	**0.05**	0.733
uLcn2/uCr (µg/mg)	0.94	0.07	**0.05**	6.665	1.00	0.00	**0.01**	24.830
uLcn2/uCr/pLcn2 (µg/mg/µg/mL)	0.97	0.04	**0.01**	2.335	1.00	0.00	**0.01**	3.879

The area under the receiver operating characteristic (ROC) curve (AUC), standard error (SE) of the AUC, the P value (vs. sham-op), and the cut-off value with the highest sensitivity and specificity are presented.

Only urinary Lcn2 discriminated successfully 10-min ischemia from the sham operation (Table 2). Furthermore, only u/pLcn2 values discriminated 10-minute ischemia from the sham operation when tested against the non-operated controls (Table 3). On the other hand, plasma Lcn2 levels and renal expression of Lcn2 mRNA discriminated only the more severe (20-min and 30-min) ischemia from sham operation (Table 2). Plasma Lcn2 levels or renal mRNA expression of Lcn2 also discriminated sham-operated from non-operated (Table 3).

Table 3. The ability of plasma and urinary Lcn2 and BUN levels to discriminate between 10-min renal ischemia and sham operation compared to non-operation (non-op) group (107).

Operation vs. non-op	**Sham-operated**				**10 min**			
Kidney damage marker	**Area**	**SE**	**P**	**Cut-off**	**Area**	**SE**	**P**	**Cut-off**
BUN (mg/dL)	0.58	0.15	0.51	N/A	0.54	0.15	0.76	N/A
Lcn2 mRNA	1.00	0.00	**0.01**	0.030	1.00	0.00	**0.001**	0.034
pLcn2 (µg/mL)	1.00	0.00	**0.001**	0.604	1.00	0.00	**0.001**	1.118
uLcn2 (µg/24h)	1.00	0.00	**0.001**	0.250	1.00	0.00	**0.001**	1.271
uLcn2/uCr (µg/mg)	1.00	0.00	**0.001**	0.775	1.00	0.00	**0.001**	4.066
uLcn2/uCr/pLcn2 (µg/mg/µg/mL)	0.53	0.10	0.81	N/A	0.88	0.06	**0.01**	2.474

The area under the receiver operating characteristic (ROC) curve (AUC), standard error (SE) of the AUC, the P value (vs. non-op), and the cut-off value with the highest sensitivity and specificity are presented.

DOI:10.14753/SE.2025.3164

5. DISCUSSION

5.1. NADPH Oxidases Are Major Contributors to Mild But Not Severe Renal Ischemia-Reperfusion Injury

We demonstrated that apocynin and neutrophil deficiency treatments protect against mild, but not moderate, or severe, renal ischemic injury (IRI). Additionally, RNAi-based knockdown of xanthine oxidoreductase (XOR) or the kidney-specific NADPH oxidase 4 (NOX4) genes did not prevent the kidney from even mild acute ischemic injury. Key findings of the therapeutic experiments are: 1) the reduction of NOX-mediated oxidative stress provides protective benefits only following mild renal ischemia-reperfusion (I/R), and 2) neutrophil deficiency also offers protection, but this effect is observed solely after mild renal I/R.

5.1.1. Progression of Functional and Morphological Damage in Ischemic Acute Kidney Injury

There is consensus regarding the role of oxidative stress in IRI (12, 111). However, various enzymes can produce reactive oxygen species (ROS) from molecular oxygen during reperfusion. The exact contribution of each ROS source to the development of renal IRI is not yet fully understood. We monitored the expression of the main enzymes of oxidative stress, such as NADPH oxidases (NOX2, NOX4, and a common NADPH oxidase subunit, $p22^{phox}$) and xanthine oxidoreductase (XOR) in the kidney. Our time-course data revealed a rapid but transient mRNA upregulation of NOX isoforms and a definite and sustained but slower increase of XOR, suggesting that these enzymes, especially NOX, may play a role in oxidative stress-related acute kidney injury (AKI). Ischemia of various durations (15, 20, and 30 min) led to renal injury of a proportional severity. The dynamics in the elevation of blood urea nitrogen (BUN) and acute tubular injury (ATI) scores indicated a progressively worsening injury after reperfusion. MPO immunohistochemistry (IHC) demonstrated that neutrophil infiltration started 3 hours post-ischemia and was extensive by 24 hours, as confirmed by mRNA expression of the macrophage marker F4/80.

Our results confirm a consecutive, two-wave oxidative stress in renal I/R. Reperfusion leads to rapid upregulation of local NOX expression, resulting in initial parenchymal damage induced by consequent oxidative stress, which triggers the recruitment of

neutrophils that infiltrate the renal interstitium. Infiltrating neutrophils contribute to a second wave of postischemic kidney injury by NOX2-mediated respiratory burst, as also shown by others in hepatic I/R (112). The most significant and extended neutrophil infiltration was detected in the outer stripe of the medulla, indicating the localization of the most severe parenchymal injury after I/R.

5.1.2. NADPH Oxidase, Not Xanthine Oxidoreductase, Mainly causes Mild Renal Ischemia-Reperfusion Injury

The inhibition of ROS production helps to reduce oxidative stress in different organs (12, 111). Primarily through its xanthine oxidase (XO) activity, XOR, as a harmful ROS producer and a source of extracellular superoxide, is considered to contribute to the inflammatory response through TLR4-mediated neutrophil activation in IRI (113). Numerous studies reported the beneficial effects of allopurinol, an XO inhibitor, by abrogating oxidative stress after renal ischemia (114). However, in our research, oxypurinol (the active metabolite of allopurinol) did not ameliorate impaired renal function. This outcome may be related to the specific action of allopurinol against its oxypurinol metabolite. Our negative findings do not support the assumption that XOR is a significant source of oxidative stress in the kidney and, consequently, reperfusion injury in mice since, in our study, neither silencing the XOR gene by RNAi nor inhibition with oxypurinol attenuated reperfusion injury, as also found by some in rats (115, 116). Additionally, the timeline of XOR upregulation and IRI pathology, as revealed in our time-course study, further supports this conclusion. In contrast to XOR inhibition, apocynin-treatment improved kidney function and morphology, but only after mild, 15-min renal ischemia. The results were similar in the groups treated with apocynin and oxypurinol, supporting that XOR inhibition was not protective. However, a recent study found that oxypurinol prevented kidney injury induced by 30-min right renal I/R and left nephrectomy (117) using the same dose and mouse strain as in our study. The authors used DMSO to dissolve oxypurinol, and DMSO is protective as reported to be beneficial in spinal cord IRI in rabbits even at the dose of 0.1 mL (118). Therefore, in that mouse study, the reported protective effect of oxypurinol could be related to the effect of DMSO itself, or a small effect of DMSO and oxypurinol could be additive, attributing a false protective effect to oxypurinol itself.

5.1.3. NADPH Oxidase Isoforms in the Pathology of Renal Ischemia-Reperfusion Injury

While there is consensus on the role of NADPH oxidases in renal oxidative stress, the contribution of specific NOX isoforms to the ROS-driven renal IRI has yet to be fully explored. Although NOX4 is the most abundant NADPH oxidase isoform in the postnatal kidney (62), other variants, such as NOX1 and NOX2, are also expressed in the tubules, glomeruli, and vasculature (119). NOX3 is only expressed in the inner ear in adult tissues (62), and NOX5 is absent in rodents (120). NOX2 (17, 121) and its close homolog NOX1 (122, 123) can generate substantial amounts of O_2, making them significant ROS sources. However, according to our data, renal NOX2 gene expression is one or two orders of magnitude lower than NOX4 or XOR. NOX2 expression can significantly increase after I/R, partly due to neutrophil infiltration, an additional source of NOX2. However, NOX2 silencing was not performed in this study as it is ineffective *in vivo* in peripheral leukocytes, such as neutrophils (124).

The abundance and constitutive activity of the H_2O_2-generating NOX4 suggest a role in oxidative stress in the kidney (125). However, knockdown by RNAi confirmed that NOX4 is not involved in the pathophysiology of renal IRI, as shown before (122).

In contrast, systemic administration of the NOX-inhibitor apocynin improved kidney function and morphology, but only after mild (15-minute) ischemia. The results were similar in the groups treated with oxypurinol plus apocynin and apocynin alone, suggesting that NOX inhibition was mainly protective. Neutrophil-derived MPO converts apocynin into active di- and trimers, which prevent $p47^{phox}$ translocation and association with other subunits of NOX complexes (126, 127). Selective inhibition of NOX1 with ML171 also ameliorated kidney function, demonstrating the involvement of vascular NOX1 in renal I/R (123). Furthermore, oxidative stress, inflammation, and fibrosis genes were downregulated in the kidneys of NOX2-deficient compared to WT mice 4 weeks after IRI (121). Our study of the neutrophil-deficient model also revealed the significant role of NOX2, which originates from neutrophil granulocytes. In summary, NOX1 and 2 isoforms are the main ROS sources in renal IRI in mice.

5.1.4. The Presumed Mechanism of NADPH Oxidase Inhibition

Nuclear factor erythroid 2-related factor 2 (NRF2) is involved in antioxidant defense by regulating the transcription of antioxidant response element (ARE) genes, e.g., heme oxygenase (HMOX)-1, NAD(P)H quinone oxidoreductase (NQO)-1, and thioredoxin reductase (TXNRD)-1 (128, 129). Hypoxia is a major factor that induces heme oxygenase 1 (HO-1) expression, which is the product of the HMOX-1 gene. HO-1, the inducible heme oxygenase isoform, plays a protective role in many renal pathologies (130). Apocynin has been found to increase NRF2 protein expression despite reducing oxidative stress (131, 132), as also observed in our study. This effect is associated with p62-dependent regulation of NRF2 expression independent of oxidative stress (133). Since NRF2 regulates HO-1 expression, apocynin can promote the nephroprotective effect of HO-1 by increasing NRF2 expression, providing a strong protective effect after I/R (128, 134). The increase in HO-1 gene expression without a change in NRF2 mRNA expression can be explained by the different expression kinetics of the two genes. NRF2 expression appeared to normalize 24 hours after mild ischemia, but postischemic HO-1 expression remained elevated. Additionally, a hindrance in NRF2 degradation may also support the maintenance of increased HO-1 expression for extended periods. Members of the glutathione peroxidase family play essential roles in antioxidant defense. glutathione peroxidase 3 (GPX3), the plasma glutathione peroxidase, has been identified as a significant biomarker of oxidative stress in renal IRI due to its strong association with oxidative stress-related, immune response-related, and apoptosis-related signaling pathways (135). The concentration of the extracellular ROS-scavenging GPX3 isoform was reduced in oxidative stress (136), as also found in this study. Treatment with apocynin restored GPX3 mRNA expression to the control level. We presume that the induction of GPX3 can be one of the antioxidant mechanisms of apocynin since GPX3 depletion induces NOX2 and can promote ROS generation (109).

5.1.5. Importance of the Severity of Renal Ischemia-Reperfusion Injury on Treatment Strategies

Our research showed that using apocynin to inhibit NOX-related oxidative stress improved kidney function and preserved kidney structure when the ischemia lasted for 15

minutes. However, when the ischemia lasted for 20 or 30 minutes, inhibiting NADPH oxidase-related oxidative stress was not protective, suggesting that cell function was so severely impaired by more extended periods of ischemia that minimizing NOX-related oxidative stress was insufficient to achieve any improvement. These results of NOX inhibition have translational relevance in the prevention of kidney damage after short ischemia, but they also point to the limitations of the protective effect of inhibiting ROS production. After prolonged ischemia, severe I/R appears to lead to predominantly NOX-independent parenchymal injury. In other words, the significance of NOX in the pathomechanism decreases with IRI severity. The complex and multifactorial nature of IRI-AKI, including various ROS sources that induce oxidative stress, inflammatory responses of both innate and adaptive immunity, ROS-induced and inflammatory damage of the capillaries leading to occlusions, and interactions between different types of regulated cell death, contribute to inconsistent research findings, making it challenging to translate experimental therapies into effective clinical treatments.

5.1.6. Neutrophils in the Pathology of Ischemic Acute Kidney Injury

The infiltrating neutrophils have a dual role in the pathology of IRI. They contribute to the postischemic inflammatory response as a part of innate immunity and are also responsible for oxidative damage via NOX2-mediated oxidative burst. Neutrophil infiltration markedly and gradually increased after reperfusion, as evidenced by MPO immunohistochemistry. Infiltration began 3 hours after reperfusion and persisted for 48 hours in the postischemic kidney (137). In our study, the NOX enzyme mRNA levels increased rapidly within 1 h after ischemia. This response was also demonstrated at protein levels in a swine I/R model and was considered complement-dependent (138). Our analysis showed that the renal NOX2, NOX4, and $p22^{phox}$ gene expression peaked at 3 hours, and a secondary increase in NOX2 expression occurred at 24 hours post-ischemia, coinciding with the peak neutrophil infiltration in the injured kidney.

The renal baseline NOX2 gene expression is lower than other oxidases (two orders of magnitude lower than NOX4 or XOR). However, there are two sources of NOX2: the local parenchymal and the phagocytic NOX2, mainly in infiltrating neutrophils. The postischemic activity of these two NOX2 populations shifted during the reperfusion period, as shown by the time course of renal NOX2 mRNA expression and MPO IHC.

This study did not perform RNAi-based silencing of the two populations of NOX2, as silencing is ineffective in peripheral leukocytes in vivo, such as neutrophils (124). The negative results after NOX4 RNAi and the positive results for apocynin point to the importance of ROS generation by infiltrating neutrophils in the pathomechanism of renal IRI. Because of their high capacity to generate superoxide, neutrophils are essential players in the pathophysiology of various diseases (139). Indeed, neutrophil-deficient chimeric mice showed strong protection against mild IRI, confirming the involvement of neutrophils in the I/R-mediated AKI. In contrast to WT animals, renal HO-1, F4/80, and TNF-α mRNA expression did not increase after I/R in neutrophil-deficient mice. As a result, GPX3 expression remained unchanged, contrary to WT mice. Apocynin produced similar effects to neutrophil deficiency. Apocynin can have two mechanisms of action. First, apocynin inhibits the local renal NADPH oxidases in the early stages of reperfusion, and second, as a result of the first mechanism, it reduces postischemic neutrophil infiltration and NOX2 activity in neutrophils. The latter protective effect may also be significant, even though the plasma concentration of apocynin decreases due to metabolism. Parenchymal NOX1/2 and phagocyte NOX2 are identified as the main contributors to mild IRI in the kidney.

5.2. Lipocalin-2 as a Biomarker of Acute Kidney Injury

We hypothesized that urinary lipocalin-2 (Lcn2) excretion or urine/plasma Lcn2 ratio could serve as a sensitive indicator of subclinical AKI, which cannot be detected using conventional markers of renal function, such as serum creatinine or blood urea nitrogen (BUN). Our results demonstrated that urinary Lcn2 excretion (uLcn2) is a sensitive and specific marker of subclinical (10-minute) renal ischemia, which is undetectable by BUN in mice. Lcn2 is similarly sensitive to BUN in detecting more severe kidney injury. Normalization of urinary Lcn2 to plasma Lcn2 (u/pLcn2) differentiates between renal and non-renal injury.

Compared to non-operated mice, renal Lcn2 mRNA expression and plasma and urinary Lcn2 protein levels were already elevated after 10 min of ischemia and proportionally increased by the duration of renal ischemia. There is growing evidence in clinical trials that plasma and urinary Lcn2 concentrations detect kidney injury before renal functional impairment can be detected by other markers (140, 141). Hence, kidney

damage markers, such as Lcn2, should be considered in addition to renal function markers for the diagnosis of subclinical AKI (142). However, further studies are needed to introduce Lcn2 into the standard clinical practice (141, 143).

A baseline of systemic Lcn2 production has been demonstrated previously (144, 145). Lcn2 is filtered by the glomeruli (144) while reabsorbed (102) and degraded (146) in proximal tubular cells (147). However, the proximal tubular capacity of Lcn2 reabsorption proved to be saturated at relatively low plasma concentrations, as evidenced by the similar intensity of Lcn2 immunostaining in the renal cortex in all groups subjected to surgery in our study. Low Lcn2 mRNA expression (by in situ hybridization) despite intense Lcn2 protein immunostaining may prove this hypothesis is true. The punctate Lcn2 staining pattern was exclusively present in the proximal tubules in the renal cortex, probably in endocytic vacuoles, suggesting Lcn2 reabsorption. As reported previously, Lcn2 immunostaining dose-dependently increased after IRI (101), similar to what we observed in our study.

Lcn2 is mainly produced by the distal tubule (89). In our study, increased renal Lcn2 production was confirmed by Lcn2 mRNA in the postischemic kidneys. Lcn2 produced in the kidney is mainly excreted in the urine, and less enters the circulation (103). These previous findings suggest that kidney injury increases renal Lcn2 excretion much more than other organ injuries. Indeed, our study demonstrated that even subclinical (10 min) renal IRI increased Lcn2 excretion more than sham operation; in contrast, plasma Lcn2 was similar after 10-minute ischemia and only elevated following mild (15 min) ischemia when compared to sham groups. In summary, this thesis section emphasizes two important conclusions regarding the clinical relevance of Lcn2 as a biomarker. First, urinary excretion of Lcn2 is identified as the most suitable biomarker for detecting subclinical AKI due to its high sensitivity. Second, the ratio of Lcn2 in plasma to urine can effectively differentiate between renal and non-renal injuries, demonstrating its specificity.

DOI:10.14753/SE.2025.3164

6. CONCLUSIONS

We demonstrated that local renal expression of NADPH oxidase (NOX) genes (NOX2, NOX4, and $p22^{phox}$) increased rapidly following renal ischemia. Xanthine oxidoreductase (XOR) expression increased slowly and remained elevated for days after ischemia-reperfusion (I/R). Renal NOX genes, but not XOR, are upregulated prior to the manifestation of the functional and morphological damage caused by I/R, indicating the primary or initiative role of the NOX rather than the XOR enzyme in the pathomechanism of renal I/R injury (IRI).

Treatment with apocynin, a NOX inhibitor, was protective in mild renal ischemia. In contrast, silencing of the NOX4 gene by RNAi did not protect the kidneys against IRI. Inhibition or silencing of the XOR enzyme/gene by oxypurinol or RNAi was also inefficient. Neutrophil-deficient $Mcl\text{-}1^{\Delta Myelo}$ mice were also protected from mild IRI, suggesting that neutrophils play a crucial role in injury following mild renal ischemia-reperfusion. Furthermore, pharmacological inhibition of reactive oxygen species (ROS) production by renal NOX enzymes with apocynin can result in a subsequent reduction in neutrophil infiltration after mild kidney damage, potentially contributing to its protective effect. Therefore, local production of ROS by renal NOX1 and NOX2 enzymes seems to play a pivotal role in reperfusion injury. Additionally, NOX2-generated ROS in neutrophils is implicated in reperfusion injury in mild (15 min) ischemic renal AKI in mice. The contribution of renal NOX1 and renal plus phagocytic NOX2 to the pathology of I/R-induced AKI is less significant after severe (20-30 min) ischemia.

Our results support the diagnostic potential of lipocalin-2 (Lcn2 or NGAL) in renal IRI and provide comprehensive data on Lcn2 in this mouse model of AKI. Plasma concentration of Lcn2 can detect renal IRI dose-dependently and with similar sensitivity to traditional markers such as blood urea nitrogen (BUN). Renal Lcn2 gene expression is similarly sensitive when used in *in vivo* animal studies. In contrast, entirely mild or very early stages of renal IRI are detected only by urinary Lcn2 excretion, even before overall renal function begins to decline. The interpretation of plasma Lcn2 concentration needs precaution (less specific), and if possible, the more sensitive and renal-specific urine excretion should be used to diagnose renal IRI. Moreover, normalization of urinary to plasma Lcn2 could help distinguish direct renal injury from extrarenal causes of Lcn2 elevation, especially if experimental circumstances require sensitive discrimination.

DOI:10.14753/SE.2025.3164

7. SUMMARY

Renal upregulation of the NADPH oxidase (NOX) family genes, but not xanthine oxidoreductase (XOR), precedes the functional and morphological signs of kidney ischemia-reperfusion (I/R) injury (IRI). NOX family members, NOX1 and NOX2 isoforms, are major contributors to mild I/R-induced acute kidney injury (AKI).

Xanthine oxidoreductase (XOR) and Renox (NOX4) are not involved in the development of renal IRI. The dynamics of neutrophil infiltration closely follow the initial damage caused by oxidative stress, leading to a subsequent secondary phase of injury characterized by reactive oxygen species production (ROS) and inflammation.

In contrast to mild renal IRI, the role of NADPH oxidase (NOX) is relatively less significant in severe AKI. This implies that as the severity of IRI increases, the contribution of NOX to the pathology decreases. In addition, the role of neutrophils remains similar in both mild and severe ischemia, their relative contribution to the pathology decreases as the severity of the ischemia increases. The complexity of this multifactorial pathomechanism presents challenges in translating experimental findings into effective treatments for renal IRI.

Urinary lipocalin-2 (Lcn2) excretion is a specific and sensitive biomarker for the diagnosis of renal IRI. Urinary Lcn2 can detect subclinical IRI or early stages of ischemic AKI, which cannot be recognized using conventional markers such as blood urea nitrogen (BUN). In addition, normalizing urinary (u) Lcn2 to plasma (p) Lcn2 levels (u/pLcn2) can help distinguish between direct renal injury and extrarenal causes of elevated plasma Lcn2 concentrations.

8. REFERENCES

1. Thomas ME, Blaine C, Dawnay A, Devonald MA, Ftouh S, Laing C, Latchem S, Lewington A, Milford DV, Ostermann M. The definition of acute kidney injury and its use in practice. Kidney Int. 2015;87(1):62-73.
2. Hoste EAJ, Kellum JA, Selby NM, Zarbock A, Palevsky PM, Bagshaw SM, Goldstein SL, Cerda J, Chawla LS. Global epidemiology and outcomes of acute kidney injury. Nat Rev Nephrol. 2018;14(10):607-625.
3. Section 2: AKI Definition. Kidney Int Suppl (2011). 2012;2(1):19-36.
4. Koeze J, Keus F, Dieperink W, van der Horst IC, Zijlstra JG, van Meurs M. Incidence, timing and outcome of AKI in critically ill patients varies with the definition used and the addition of urine output criteria. BMC Nephrol. 2017;18(1):70.
5. Jentzer JC, Breen T, Sidhu M, Barsness GW, Kashani K. Epidemiology and outcomes of acute kidney injury in cardiac intensive care unit patients. J Crit Care. 2020;60:127-134.
6. Kellum JA, Romagnani P, Ashuntantang G, Ronco C, Zarbock A, Anders HJ. Acute kidney injury. Nat Rev Dis Primers. 2021;7(1):52.
7. Mo S, Bjelland TW, Nilsen TIL, Klepstad P. Acute kidney injury in intensive care patients: Incidence, time course, and risk factors. Acta Anaesthesiol Scand. 2022;66(8):961-968.
8. Basile DP, Anderson MD, Sutton TA. Pathophysiology of acute kidney injury. Compr Physiol. 2012;2(2):1303-1353.
9. He L, Wei Q, Liu J, Yi M, Liu Y, Liu H, Sun L, Peng Y, Liu F, Venkatachalam MA, Dong Z. AKI on CKD: heightened injury, suppressed repair, and the underlying mechanisms. Kidney Int. 2017;92(5):1071-1083.
10. Han SJ, Lee HT. Mechanisms and therapeutic targets of ischemic acute kidney injury. Kidney Res Clin Pract. 2019;38(4):427-440.
11. Eltzschig HK, Eckle T. Ischemia and reperfusion--from mechanism to translation. Nat Med. 2011;17(11):1391-1401.
12. Granata S, Votrico V, Spadaccino F, Catalano V, Netti GS, Ranieri E, Stallone G, Zaza G. Oxidative Stress and Ischemia/Reperfusion Injury in Kidney Transplantation: Focus on Ferroptosis, Mitophagy and New Antioxidants. Antioxidants (Basel). 2022;11(4).
13. Pabla N, Bajwa A. Role of Mitochondrial Therapy for Ischemic-Reperfusion Injury and Acute Kidney Injury. Nephron. 2022;146(3):253-258.

14. Wu MY, Yiang GT, Liao WT, Tsai AP, Cheng YL, Cheng PW, Li CY, Li CJ. Current Mechanistic Concepts in Ischemia and Reperfusion Injury. Cell Physiol Biochem. 2018;46(4):1650-1667.
15. Kaushal GP, Chandrashekar K, Juncos LA. Molecular Interactions Between Reactive Oxygen Species and Autophagy in Kidney Disease. Int J Mol Sci. 2019;20(15).
16. McCord JM. Oxygen-derived free radicals in postischemic tissue injury. N Engl J Med. 1985;312(3):159-163.
17. Bedard K, Krause KH. The NOX family of ROS-generating NADPH oxidases: physiology and pathophysiology. Physiol Rev. 2007;87(1):245-313.
18. Kinsey GR, Li L, Okusa MD. Inflammation in acute kidney injury. Nephron Exp Nephrol. 2008;109(4):e102-107.
19. Salvadori M, Rosso G, Bertoni E. Update on ischemia-reperfusion injury in kidney transplantation: Pathogenesis and treatment. World J Transplant. 2015;5(2):52-67.
20. Noiri E, Nakao A, Uchida K, Tsukahara H, Ohno M, Fujita T, Brodsky S, Goligorsky MS. Oxidative and nitrosative stress in acute renal ischemia. Am J Physiol Renal Physiol. 2001;281(5):F948-957.
21. Lee S, Huen S, Nishio H, Nishio S, Lee HK, Choi BS, Ruhrberg C, Cantley LG. Distinct macrophage phenotypes contribute to kidney injury and repair. J Am Soc Nephrol. 2011;22(2):317-326.
22. Meng XM, Tang PM, Li J, Lan HY. Macrophage Phenotype in Kidney Injury and Repair. Kidney Dis (Basel). 2015;1(2):138-146.
23. Bouchery T, Harris N. Neutrophil-macrophage cooperation and its impact on tissue repair. Immunol Cell Biol. 2019;97(3):289-298.
24. Tonnus W, Meyer C, Steinebach C, Belavgeni A, von Massenhausen A, Gonzalez NZ, Maremonti F, Gembardt F, Himmerkus N, Latk M, Locke S, Marschner J, Li W, Short S, Doll S, Ingold I, Proneth B, Daniel C, Kabgani N, Kramann R, Motika S, Hergenrother PJ, Bornstein SR, Hugo C, Becker JU, Amann K, Anders HJ, Kreisel D, Pratt D, Gutschow M, Conrad M, Linkermann A. Dysfunction of the key ferroptosis-surveilling systems hypersensitizes mice to tubular necrosis during acute kidney injury. Nat Commun. 2021;12(1):4402.
25. Winterberg PD, Lu CY. Acute kidney injury: the beginning of the end of the dark ages. Am J Med Sci. 2012;344(4):318-325.
26. Bonventre JV, Yang L. Cellular pathophysiology of ischemic acute kidney injury. J Clin Invest. 2011;121(11):4210-4221.

27. Kwiatkowska E, Kwiatkowski S, Dziedziejko V, Tomasiewicz I, Domanski L. Renal Microcirculation Injury as the Main Cause of Ischemic Acute Kidney Injury Development. Biology (Basel). 2023;12(2).
28. Patschan D, Patschan S, Muller GA. Inflammation and microvasculopathy in renal ischemia reperfusion injury. J Transplant. 2012;2012:764154.
29. Lazzeri E, Angelotti ML, Peired A, Conte C, Marschner JA, Maggi L, Mazzinghi B, Lombardi D, Melica ME, Nardi S, Ronconi E, Sisti A, Antonelli G, Becherucci F, De Chiara L, Guevara RR, Burger A, Schaefer B, Annunziato F, Anders HJ, Lasagni L, Romagnani P. Endocycle-related tubular cell hypertrophy and progenitor proliferation recover renal function after acute kidney injury. Nat Commun. 2018;9(1):1344.
30. Mulay SR, Linkermann A, Anders HJ. Necroinflammation in Kidney Disease. J Am Soc Nephrol. 2016;27(1):27-39.
31. Schnaper HW. Remnant nephron physiology and the progression of chronic kidney disease. Pediatr Nephrol. 2014;29(2):193-202.
32. Sharma M, Singh V, Sharma R, Koul A, McCarthy ET, Savin VJ, Joshi T, Srivastava T. Glomerular Biomechanical Stress and Lipid Mediators during Cellular Changes Leading to Chronic Kidney Disease. Biomedicines. 2022;10(2).
33. Droge W. Free radicals in the physiological control of cell function. Physiol Rev. 2002;82(1):47-95.
34. Ratliff BB, Abdulmahdi W, Pawar R, Wolin MS. Oxidant Mechanisms in Renal Injury and Disease. Antioxid Redox Signal. 2016;25(3):119-146.
35. Wu L, Xiong X, Wu X, Ye Y, Jian Z, Zhi Z, Gu L. Targeting Oxidative Stress and Inflammation to Prevent Ischemia-Reperfusion Injury. Front Mol Neurosci. 2020;13:28.
36. Granger DN, Kvietys PR. Reperfusion injury and reactive oxygen species: The evolution of a concept. Redox Biol. 2015;6:524-551.
37. Di Meo S, Reed TT, Venditti P, Victor VM. Role of ROS and RNS Sources in Physiological and Pathological Conditions. Oxid Med Cell Longev. 2016;2016:1245049.
38. Babior BM. NADPH oxidase. Curr Opin Immunol. 2004;16(1):42-47.
39. Babior BM, Lambeth JD, Nauseef W. The neutrophil NADPH oxidase. Arch Biochem Biophys. 2002;397(2):342-344.
40. Ushio-Fukai M, Zafari AM, Fukui T, Ishizaka N, Griendling KK. p22phox is a critical component of the superoxide-generating NADH/NADPH oxidase system and regulates angiotensin II-induced hypertrophy in vascular smooth muscle cells. J Biol Chem. 1996;271(38):23317-23321.

41. Panday A, Sahoo MK, Osorio D, Batra S. NADPH oxidases: an overview from structure to innate immunity-associated pathologies. Cell Mol Immunol. 2015;12(1):5-23.
42. Stasia MJ. CYBA encoding p22(phox), the cytochrome b558 alpha polypeptide: gene structure, expression, role and physiopathology. Gene. 2016;586(1):27-35.
43. Royer-Pokora B, Kunkel LM, Monaco AP, Goff SC, Newburger PE, Baehner RL, Cole FS, Curnutte JT, Orkin SH. Cloning the gene for an inherited human disorder--chronic granulomatous disease--on the basis of its chromosomal location. Nature. 1986;322(6074):32-38.
44. Quinn MT, Parkos CA, Walker L, Orkin SH, Dinauer MC, Jesaitis AJ. Association of a Ras-related protein with cytochrome b of human neutrophils. Nature. 1989;342(6246):198-200.
45. Vermot A, Petit-Hartlein I, Smith SME, Fieschi F. NADPH Oxidases (NOX): An Overview from Discovery, Molecular Mechanisms to Physiology and Pathology. Antioxidants (Basel, Switzerland). 2021;10(6).
46. Altenhofer S, Radermacher KA, Kleikers PW, Wingler K, Schmidt HH. Evolution of NADPH Oxidase Inhibitors: Selectivity and Mechanisms for Target Engagement. Antioxid Redox Signal. 2015;23(5):406-427.
47. Geiszt M, Kopp JB, Varnai P, Leto TL. Identification of renox, an NAD(P)H oxidase in kidney. Proc Natl Acad Sci U S A. 2000;97(14):8010-8014.
48. Martyn KD, Frederick LM, von Loehneysen K, Dinauer MC, Knaus UG. Functional analysis of Nox4 reveals unique characteristics compared to other NADPH oxidases. Cell Signal. 2006;18(1):69-82.
49. Block K, Gorin Y, Abboud HE. Subcellular localization of Nox4 and regulation in diabetes. Proc Natl Acad Sci U S A. 2009;106(34):14385-14390.
50. Takac I, Schroder K, Zhang L, Lardy B, Anilkumar N, Lambeth JD, Shah AM, Morel F, Brandes RP. The E-loop is involved in hydrogen peroxide formation by the NADPH oxidase Nox4. The Journal of biological chemistry. 2011;286(15):13304-13313.
51. Nisimoto Y, Diebold BA, Cosentino-Gomes D, Lambeth JD. Nox4: a hydrogen peroxide-generating oxygen sensor. Biochemistry. 2014;53(31):5111-5120.
52. Chen F, Haigh S, Barman S, Fulton DJ. From form to function: the role of Nox4 in the cardiovascular system. Front Physiol. 2012;3:412.
53. Lambeth JD, Neish AS. Nox enzymes and new thinking on reactive oxygen: a double-edged sword revisited. Annu Rev Pathol. 2014;9:119-145.
54. Morawietz H. Endothelial NADPH oxidases: friends or foes? Basic Res Cardiol. 2011;106(4):521-525.

55. Suh YA, Arnold RS, Lassegue B, Shi J, Xu X, Sorescu D, Chung AB, Griendling KK, Lambeth JD. Cell transformation by the superoxide-generating oxidase Mox1. Nature. 1999;401(6748):79-82.
56. Geiszt M, Lekstrom K, Brenner S, Hewitt SM, Dana R, Malech HL, Leto TL. NAD(P)H oxidase 1, a product of differentiated colon epithelial cells, can partially replace glycoprotein 91phox in the regulated production of superoxide by phagocytes. J Immunol. 2003;171(1):299-306.
57. Katsuyama M, Fan C, Yabe-Nishimura C. NADPH oxidase is involved in prostaglandin F2alpha-induced hypertrophy of vascular smooth muscle cells: induction of NOX1 by PGF2alpha. The Journal of biological chemistry. 2002;277(16):13438-13442.
58. Lassegue B, Sorescu D, Szocs K, Yin Q, Akers M, Zhang Y, Grant SL, Lambeth JD, Griendling KK. Novel gp91(phox) homologues in vascular smooth muscle cells: nox1 mediates angiotensin II-induced superoxide formation and redox-sensitive signaling pathways. Circ Res. 2001;88(9):888-894.
59. Banfi B, Malgrange B, Knisz J, Steger K, Dubois-Dauphin M, Krause K-H. NOX3, a superoxide-generating NADPH oxidase of the inner ear. The Journal of biological chemistry. 2004;279(44):46065-46072.
60. Paffenholz R, Bergstrom RA, Pasutto F, Wabnitz P, Munroe RJ, Jagla W, Heinzmann U, Marquardt A, Bareiss A, Laufs J, Russ A, Stumm G, Schimenti JC, Bergstrom DE. Vestibular defects in head-tilt mice result from mutations in Nox3, encoding an NADPH oxidase. Genes Dev. 2004;18(5):486-491.
61. Downs CA, Helms MN. Regulation of ion transport by oxidants. Am J Physiol Lung Cell Mol Physiol. 2013;305(9):L595-603.
62. Cheng G, Cao Z, Xu X, van Meir EG, Lambeth JD. Homologs of gp91phox: cloning and tissue expression of Nox3, Nox4, and Nox5. Gene. 2001;269(1-2):131-140.
63. Nazari B, Jaquet V, Krause KH. NOX family NADPH oxidases in mammals: Evolutionary conservation and isoform-defining sequences. Redox Biol. 2023;66:102851.
64. Banfi B, Tirone F, Durussel I, Knisz J, Moskwa P, Molnar GZ, Krause K-H, Cox JA. Mechanism of Ca2+ activation of the NADPH oxidase 5 (NOX5). The Journal of biological chemistry. 2004;279(18):18583-18591.
65. Reyes-San-Martin C, Hamoh T, Zhang Y, Berendse L, Klijn C, Li R, Llumbet AE, Sigaeva A, Kawalko J, Mzyk A, Schirhagl R. Nanoscale MRI for Selective Labeling and Localized Free Radical Measurements in the Acrosomes of Single Sperm Cells. ACS Nano. 2022;16(7):10701-10710.

66. Grasberger H, Refetoff S. Identification of the maturation factor for dual oxidase. Evolution of an eukaryotic operon equivalent. J Biol Chem. 2006;281(27):18269-18272.
67. Morand S, Ueyama T, Tsujibe S, Saito N, Korzeniowska A, Leto TL. Duox maturation factors form cell surface complexes with Duox affecting the specificity of reactive oxygen species generation. FASEB J. 2009;23(4):1205-1218.
68. Harrison R. Structure and function of xanthine oxidoreductase: where are we now? Free Radic Biol Med. 2002;33(6):774-797.
69. Saksela M, Lapatto R, Raivio KO. Xanthine oxidoreductase gene expression and enzyme activity in developing human tissues. Biol Neonate. 1998;74(4):274-280.
70. Nishino T, Okamoto K, Eger BT, Pai EF, Nishino T. Mammalian xanthine oxidoreductase - mechanism of transition from xanthine dehydrogenase to xanthine oxidase. Febs J. 2008;275(13):3278-3289.
71. Olson JS, Ballou DP, Palmer G, Massey V. The mechanism of action of xanthine oxidase. J Biol Chem. 1974;249(14):4363-4382.
72. Kobayashi K, Miki M, Okamoto K, Nishino T. Electron transfer process in milk xanthine dehydrogenase as studied by pulse radiolysis. J Biol Chem. 1993;268(33):24642-24646.
73. Komai H, Massey V, Palmer G. The preparation and properties of deflavo xanthine oxidase. J Biol Chem. 1969;244(7):1692-1700.
74. Kanda M, Brady FO, Rajagopalan KV, Handler P. Studies on the dissociation of flavin adenine dinucleotide from metalloflavoproteins. J Biol Chem. 1972;247(3):765-770.
75. Bortolotti M, Polito L, Battelli MG, Bolognesi A. Xanthine oxidoreductase: One enzyme for multiple physiological tasks. Redox Biol. 2021;41:101882.
76. Cantu-Medellin N, Kelley EE. Xanthine oxidoreductase-catalyzed reactive species generation: A process in critical need of reevaluation. Redox Biol. 2013;1(1):353-358.
77. Hille R, Nishino T. Flavoprotein structure and mechanism. 4. Xanthine oxidase and xanthine dehydrogenase. FASEB J. 1995;9(11):995-1003.
78. McNally JS, Saxena A, Cai H, Dikalov S, Harrison DG. Regulation of xanthine oxidoreductase protein expression by hydrogen peroxide and calcium. Arterioscler Thromb Vasc Biol. 2005;25(8):1623-1628.
79. Flemmig J, Kuchta K, Arnhold J, Rauwald HW. Olea europaea leaf (Ph.Eur.) extract as well as several of its isolated phenolics inhibit the gout-related enzyme xanthine oxidase. Phytomedicine. 2011;18(7):561-566.

80. Adamus JP, Ruszczynska A, Wyczalkowska-Tomasik A. Molybdenum's Role as an Essential Element in Enzymes Catabolizing Redox Reactions: A Review. Biomolecules. 2024;14(7).
81. Franzin R, Stasi A, Fiorentino M, Simone S, Oberbauer R, Castellano G, Gesualdo L. Renal Delivery of Pharmacologic Agents During Machine Perfusion to Prevent Ischaemia-Reperfusion Injury: From Murine Model to Clinical Trials. Front Immunol. 2021;12:673562.
82. Andreucci M, Faga T, Pisani A, Perticone M, Michael A. The ischemic/nephrotoxic acute kidney injury and the use of renal biomarkers in clinical practice. Eur J Intern Med. 2017;39:1-8.
83. Ostermann M, Legrand M, Meersch M, Srisawat N, Zarbock A, Kellum JA. Biomarkers in acute kidney injury. Ann Intensive Care. 2024;14(1):145.
84. Tsuji K, Nakanoh H, Fukushima K, Kitamura S, Wada J. MicroRNAs as Biomarkers and Therapeutic Targets for Acute Kidney Injury. Diagnostics (Basel). 2023;13(18).
85. Wu YL, Li HF, Chen HH, Lin H. MicroRNAs as Biomarkers and Therapeutic Targets in Inflammation- and Ischemia-Reperfusion-Related Acute Renal Injury. Int J Mol Sci. 2020;21(18).
86. Bakinowska E, Kielbowski K, Pawlik A. The Role of MicroRNA in the Pathogenesis of Acute Kidney Injury. Cells. 2024;13(18).
87. Liu Z, Fu Y, Yan M, Zhang S, Cai J, Chen G, Dong Z. microRNAs in kidney diseases: Regulation, therapeutics, and biomarker potential. Pharmacol Ther. 2024;262:108709.
88. Kaucsar T, Revesz C, Godo M, Krenacs T, Albert M, Szalay CI, Rosivall L, Benyo Z, Batkai S, Thum T, Szenasi G, Hamar P. Activation of the miR-17 family and miR-21 during murine kidney ischemia-reperfusion injury. Nucleic Acid Ther. 2013;23(5):344-354.
89. Paragas N, Qiu A, Zhang Q, Samstein B, Deng SX, Schmidt-Ott KM, Viltard M, Yu W, Forster CS, Gong G, Liu Y, Kulkarni R, Mori K, Kalandadze A, Ratner AJ, Devarajan P, Landry DW, D'Agati V, Lin CS, Barasch J. The Ngal reporter mouse detects the response of the kidney to injury in real time. Nat Med. 2011;17(2):216-222.
90. Mishra J, Ma Q, Prada A, Mitsnefes M, Zahedi K, Yang J, Barasch J, Devarajan P. Identification of neutrophil gelatinase-associated lipocalin as a novel early urinary biomarker for ischemic renal injury. J Am Soc Nephrol. 2003;14(10):2534-2543.
91. Mishra J, Dent C, Tarabishi R, Mitsnefes MM, Ma Q, Kelly C, Ruff SM, Zahedi K, Shao M, Bean J, Mori K, Barasch J, Devarajan P. Neutrophil gelatinase-associated

lipocalin (NGAL) as a biomarker for acute renal injury after cardiac surgery. Lancet. 2005;365(9466):1231-1238.

92. Singer E, Marko L, Paragas N, Barasch J, Dragun D, Muller DN, Budde K, Schmidt-Ott KM. Neutrophil gelatinase-associated lipocalin: pathophysiology and clinical applications. Acta Physiol (Oxf). 2013;207(4):663-672.
93. Haase-Fielitz A, Haase M, Devarajan P. Neutrophil gelatinase-associated lipocalin as a biomarker of acute kidney injury: a critical evaluation of current status. Ann Clin Biochem. 2014;51(Pt 3):335-351.
94. Hjortrup PB, Haase N, Wetterslev M, Perner A. Clinical review: Predictive value of neutrophil gelatinase-associated lipocalin for acute kidney injury in intensive care patients. Crit Care. 2013;17(2):211.
95. Munshi R, Johnson A, Siew ED, Ikizler TA, Ware LB, Wurfel MM, Himmelfarb J, Zager RA. MCP-1 gene activation marks acute kidney injury. J Am Soc Nephrol. 2011;22(1):165-175.
96. Cai L, Rubin J, Han W, Venge P, Xu S. The origin of multiple molecular forms in urine of HNL/NGAL. Clin J Am Soc Nephrol. 2010;5(12):2229-2235.
97. Lacquaniti A, Buemi F, Lupica R, Giardina C, Mure G, Arena A, Visalli C, Baldari S, Aloisi C, Buemi M. Can neutrophil gelatinase-associated lipocalin help depict early contrast material-induced nephropathy? Radiology. 2013;267(1):86-93.
98. Liu Q, Nilsen-Hamilton M. Identification of a new acute phase protein. J Biol Chem. 1995;270(38):22565-22570.
99. Nielsen BS, Borregaard N, Bundgaard JR, Timshel S, Sehested M, Kjeldsen L. Induction of NGAL synthesis in epithelial cells of human colorectal neoplasia and inflammatory bowel diseases. Gut. 1996;38(3):414-420.
100. Cowland JB, Sorensen OE, Sehested M, Borregaard N. Neutrophil gelatinase-associated lipocalin is up-regulated in human epithelial cells by IL-1 beta, but not by TNF-alpha. J Immunol. 2003;171(12):6630-6639.
101. Friedl A, Stoesz SP, Buckley P, Gould MN. Neutrophil gelatinase-associated lipocalin in normal and neoplastic human tissues. Cell type-specific pattern of expression. Histochem J. 1999;31(7):433-441.
102. Kuwabara T, Mori K, Mukoyama M, Kasahara M, Yokoi H, Saito Y, Yoshioka T, Ogawa Y, Imamaki H, Kusakabe T, Ebihara K, Omata M, Satoh N, Sugawara A, Barasch J, Nakao K. Urinary neutrophil gelatinase-associated lipocalin levels reflect damage to glomeruli, proximal tubules, and distal nephrons. Kidney Int. 2009;75(3):285-294.

103. Schmidt-Ott KM, Mori K, Li JY, Kalandadze A, Cohen DJ, Devarajan P, Barasch J. Dual action of neutrophil gelatinase-associated lipocalin. J Am Soc Nephrol. 2007;18(2):407-413.
104. Weber FC, Nemeth T, Csepregi JZ, Dudeck A, Roers A, Ozsvari B, Oswald E, Puskas LG, Jakob T, Mocsai A, Martin SF. Neutrophils are required for both the sensitization and elicitation phase of contact hypersensitivity. J Exp Med. 2015;212(1):15-22.
105. Csepregi JZ, Orosz A, Zajta E, Kasa O, Nemeth T, Simon E, Fodor S, Csonka K, Baratki BL, Kovesdi D, He YW, Gacser A, Mocsai A. Myeloid-Specific Deletion of Mcl-1 Yields Severely Neutropenic Mice That Survive and Breed in Homozygous Form. J Immunol. 2018;201(12):3793-3803.
106. Hamar P, Song E, Kokeny G, Chen A, Ouyang N, Lieberman J. Small interfering RNA targeting Fas protects mice against renal ischemia-reperfusion injury. Proc Natl Acad Sci U S A. 2004;101(41):14883-14888.
107. Kaucsar T, Godo M, Revesz C, Kovacs M, Mocsai A, Kiss N, Albert M, Krenacs T, Szenasi G, Hamar P. Urine/Plasma Neutrophil Gelatinase Associated Lipocalin Ratio Is a Sensitive and Specific Marker of Subclinical Acute Kidney Injury in Mice. PLoS One. 2016;11(1):e0148043.
108. Revesz C, Kaucsar T, Godo M, Bocskai K, Krenacs T, Mocsai A, Szenasi G, Hamar P. Neutrophils and NADPH Oxidases Are Major Contributors to Mild but Not Severe Ischemic Acute Kidney Injury in Mice. Int J Mol Sci. 2024;25(5).
109. Li L, He M, Tang X, Huang J, Li J, Hong X, Fu H, Liu Y. Proteomic landscape of the extracellular matrix in the fibrotic kidney. Kidney Int. 2023;103(6):1063-1076.
110. Hamada S, Takata T, Yamada K, Yamamoto M, Mae Y, Iyama T, Ikeda S, Kanda T, Sugihara T, Isomoto H. Steatosis is involved in the progression of kidney disease in a high-fat-diet-induced non-alcoholic steatohepatitis mouse model. PLoS One. 2022;17(3):e0265461.
111. Chazelas P, Steichen C, Favreau F, Trouillas P, Hannaert P, Thuillier R, Giraud S, Hauet T, Guillard J. Oxidative Stress Evaluation in Ischemia Reperfusion Models: Characteristics, Limits and Perspectives. Int J Mol Sci. 2021;22(5).
112. Mukhopadhyay P, Horvath B, Zsengeller Z, Batkai S, Cao Z, Kechrid M, Holovac E, Erdelyi K, Tanchian G, Liaudet L, Stillman IE, Joseph J, Kalyanaraman B, Pacher P. Mitochondrial reactive oxygen species generation triggers inflammatory response and tissue injury associated with hepatic ischemia-reperfusion: therapeutic potential of mitochondrially targeted antioxidants. Free Radic Biol Med. 2012;53(5):1123-1138.

113. Al-Khafaji AB, Tohme S, Yazdani HO, Miller D, Huang H, Tsung A. Superoxide induces Neutrophil Extracellular Trap Formation in a TLR-4 and NOX-dependent mechanism. Mol Med. 2016;22:621-631.
114. Prieto-Moure B, Caraben-Redano A, Aliena-Valero A, Cejalvo D, Toledo AH, Flores-Bellver M, Martinez-Gil N, Toledo-Pereyra LH, Lloris Carsi JM. Allopurinol in renal ischemia. J Invest Surg. 2014;27(5):304-316.
115. Zager RA, Fuerstenberg SM, Baehr PH, Myerson D, Torok-Storb B. An evaluation of antioxidant effects on recovery from postischemic acute renal failure. J Am Soc Nephrol. 1994;4(8):1588-1597.
116. Radovic M, Miloradovic Z, Popovic T, Mihailovic-Stanojevic N, Jovovic D, Tomovic M, Colak E, Simic-Ogrizovic S, Djukanovic L. Allopurinol and enalapril failed to conserve urinary NOx and sodium in ischemic acute renal failure in spontaneously hypertensive rats. Am J Nephrol. 2006;26(4):388-399.
117. Kang HB, Lim CK, Kim J, Han SJ. Oxypurinol protects renal ischemia/reperfusion injury via heme oxygenase-1 induction. Front Med (Lausanne). 2023;10:1030577.
118. Turan NN, Akar F, Budak B, Seren M, Parlar AI, Surucu S, Ulus AT. How DMSO, a widely used solvent, affects spinal cord injury. Ann Vasc Surg. 2008;22(1):98-105.
119. Holterman CE, Read NC, Kennedy CR. Nox and renal disease. Clin Sci (Lond). 2015;128(8):465-481.
120. Touyz RM, Anagnostopoulou A, Rios F, Montezano AC, Camargo LL. NOX5: Molecular biology and pathophysiology. Exp Physiol. 2019;104(5):605-616.
121. Karim AS, Reese SR, Wilson NA, Jacobson LM, Zhong W, Djamali A. Nox2 is a mediator of ischemia reperfusion injury. Am J Transplant. 2015;15(11):2888-2899.
122. Munoz M, Lopez-Oliva ME, Rodriguez C, Martinez MP, Saenz-Medina J, Sanchez A, Climent B, Benedito S, Garcia-Sacristan A, Rivera L, Hernandez M, Prieto D. Differential contribution of Nox1, Nox2 and Nox4 to kidney vascular oxidative stress and endothelial dysfunction in obesity. Redox Biol. 2020;28:101330.
123. Jung HY, Oh SH, Ahn JS, Oh EJ, Kim YJ, Kim CD, Park SH, Kim YL, Cho JH. NOX1 Inhibition Attenuates Kidney Ischemia-Reperfusion Injury via Inhibition of ROS-Mediated ERK Signaling. Int J Mol Sci. 2020;21(18).
124. Peer D, Zhu P, Carman CV, Lieberman J, Shimaoka M. Selective gene silencing in activated leukocytes by targeting siRNAs to the integrin lymphocyte function-associated antigen-1. Proc Natl Acad Sci U S A. 2007;104(10):4095-4100.
125. Brandes RP, Takac I, Schroder K. No superoxide--no stress?: Nox4, the good NADPH oxidase! Arterioscler Thromb Vasc Biol. 2011;31(6):1255-1257.

126. Boshtam M, Kouhpayeh S, Amini F, Azizi Y, Najaflu M, Shariati L, Khanahmad H. Anti-inflammatory effects of apocynin: a narrative review of the evidence. All Life. 2021;14(1):997-1010.
127. Kim JY, Park J, Lee JE, Yenari MA. NOX Inhibitors - A Promising Avenue for Ischemic Stroke. Exp Neurobiol. 2017;26(4):195-205.
128. Nezu M, Suzuki N. Roles of Nrf2 in Protecting the Kidney from Oxidative Damage. Int J Mol Sci. 2020;21(8).
129. Potteti HR, Noone PM, Tamatam CR, Ankireddy A, Noel S, Rabb H, Reddy SP. Nrf2 mediates hypoxia-inducible HIF1alpha activation in kidney tubular epithelial cells. Am J Physiol Renal Physiol. 2021;320(3):F464-F474.
130. Grunenwald A, Roumenina LT, Frimat M. Heme Oxygenase 1: A Defensive Mediator in Kidney Diseases. Int J Mol Sci. 2021;22(4).
131. Bhatt NP, Park JY, Lee HJ, Kim SS, Kwon YS, Chun W. Apocynin protects mesangial cells from lipopolysaccharide-induced inflammation by exerting heme oxygenase 1-mediated monocyte chemoattractant protein-1 suppression. Int J Mol Med. 2017;40(4):1294-1301.
132. Mahmoud NA, Hassanein EHM, Bakhite EA, Shaltout ES, Sayed AM. Apocynin and its chitosan nanoparticles attenuated cisplatin-induced multiorgan failure: Synthesis, characterization, and biological evaluation. Life Sci. 2023;314:121313.
133. Baird L, Yamamoto M. The Molecular Mechanisms Regulating the KEAP1-NRF2 Pathway. Mol Cell Biol. 2020;40(13).
134. Guerrero-Hue M, Rayego-Mateos S, Vazquez-Carballo C, Palomino-Antolin A, Garcia-Caballero C, Opazo-Rios L, Morgado-Pascual JL, Herencia C, Mas S, Ortiz A, Rubio-Navarro A, Egea J, Villalba JM, Egido J, Moreno JA. Protective Role of Nrf2 in Renal Disease. Antioxidants (Basel). 2020;10(1).
135. Pei J, Tian X, Yu C, Luo J, Zhang J, Hua Y, Wei G. GPX3 and GSTT1 as biomarkers related to oxidative stress during renal ischemia reperfusion injuries and their relationship with immune infiltration. Front Immunol. 2023;14:1136146.
136. Wu Y, Shi H, Xu Y, Wen R, Gong M, Hong G, Xu S. Selenoprotein Gene mRNA Expression Evaluation During Renal Ischemia-Reperfusion Injury in Rats and Ebselen Intervention Effects. Biol Trace Elem Res. 2023;201(4):1792-1805.
137. Awad AS, Rouse M, Huang L, Vergis AL, Reutershan J, Cathro HP, Linden J, Okusa MD. Compartmentalization of neutrophils in the kidney and lung following acute ischemic kidney injury. Kidney Int. 2009;75(7):689-698.
138. Simone S, Rascio F, Castellano G, Divella C, Chieti A, Ditonno P, Battaglia M, Crovace A, Staffieri F, Oortwijn B, Stallone G, Gesualdo L, Pertosa G, Grandaliano

G. Complement-dependent NADPH oxidase enzyme activation in renal ischemia/reperfusion injury. Free Radic Biol Med. 2014;74:263-273.

139. Nemeth T, Sperandio M, Mocsai A. Neutrophils as emerging therapeutic targets. Nat Rev Drug Discov. 2020;19(4):253-275.
140. Haase M, Devarajan P, Haase-Fielitz A, Bellomo R, Cruz DN, Wagener G, Krawczeski CD, Koyner JL, Murray P, Zappitelli M, Goldstein SL, Makris K, Ronco C, Martensson J, Martling CR, Venge P, Siew E, Ware LB, Ikizler TA, Mertens PR. The outcome of neutrophil gelatinase-associated lipocalin-positive subclinical acute kidney injury: a multicenter pooled analysis of prospective studies. J Am Coll Cardiol. 2011;57(17):1752-1761.
141. Clerico A, Galli C, Fortunato A, Ronco C. Neutrophil gelatinase-associated lipocalin (NGAL) as biomarker of acute kidney injury: a review of the laboratory characteristics and clinical evidences. Clin Chem Lab Med. 2012;50(9):1505-1517.
142. McCullough PA, Shaw AD, Haase M, Bouchard J, Waikar SS, Siew ED, Murray PT, Mehta RL, Ronco C. Diagnosis of acute kidney injury using functional and injury biomarkers: workgroup statements from the tenth Acute Dialysis Quality Initiative Consensus Conference. Contrib Nephrol. 2013;182:13-29.
143. Murray PT, Mehta RL, Shaw A, Ronco C, Endre Z, Kellum JA, Chawla LS, Cruz D, Ince C, Okusa MD, workgroup A. Potential use of biomarkers in acute kidney injury: report and summary of recommendations from the 10th Acute Dialysis Quality Initiative consensus conference. Kidney Int. 2014;85(3):513-521.
144. Axelsson L, Bergenfeldt M, Ohlsson K. Studies of the release and turnover of a human neutrophil lipocalin. Scand J Clin Lab Invest. 1995;55(7):577-588.
145. Paragas N, Qiu A, Hollmen M, Nickolas TL, Devarajan P, Barasch J. NGAL-Siderocalin in kidney disease. Biochim Biophys Acta. 2012;1823(9):1451-1458.
146. Mori K, Lee HT, Rapoport D, Drexler IR, Foster K, Yang J, Schmidt-Ott KM, Chen X, Li JY, Weiss S, Mishra J, Cheema FH, Markowitz G, Suganami T, Sawai K, Mukoyama M, Kunis C, D'Agati V, Devarajan P, Barasch J. Endocytic delivery of lipocalin-siderophore-iron complex rescues the kidney from ischemia-reperfusion injury. J Clin Invest. 2005;115(3):610-621.
147. Hvidberg V, Jacobsen C, Strong RK, Cowland JB, Moestrup SK, Borregaard N. The endocytic receptor megalin binds the iron transporting neutrophil-gelatinase-associated lipocalin with high affinity and mediates its cellular uptake. FEBS Lett. 2005;579(3):773-777.

9. BIBLIOGRAPHY OF THE CANDIDATE'S PUBLICATIONS

9.1. Related to the PhD Thesis

1. **Révész C**, Kaucsár T, Godó M, Bocskai K, Krenács T, Mócsai A, Szénási G, Hamar P. Neutrophils and NADPH Oxidases Are Major Contributors to Mild but Not Severe Ischemic Acute Kidney Injury in Mice. Int J Mol Sci. 2024;25(5):2948.
2. Kaucsár T, Godó M, **Révész C,** Kovács M, Mócsai A, Kiss N, Albert M, Krenács T, Szénási G, Hamar P: Urine/Plasma Neutrophil Gelatinase Associated Lipocalin Ratio Is a Sensitive and Specific Marker of Subclinical Acute Kidney Injury in Mice. PLoS One. 2016;11(1):e0148043.

9.2. Unrelated to the PhD Thesis

1. Pethő ÁG, **Révész C**, Mészáros T, Sáfár O, Rosivall L, Domán J, Szénási G, Gigacz T, Dézsi L. Pathophysiological changes in patients during hemodialysis and blood reinfusion predict potential development of hemodialysis reactions. Renal Failure. 2025;47(1):2500662.
2. **Révész C**, Wasik AA, Godó M, Tod P, Lehtonen S, Szénási G, Hamar P: Cold Saline Perfusion before Ischemia-Reperfusion Is Harmful to the Kidney and Is Associated with the Loss of Ezrin, a Cytoskeletal Protein, in Rats. Biomedicines. 2021;9(1):30.
3. Kökény G, Fang L, **Révész C**, Rosivall L: The Effect of Combined Treatment with the (Pro)Renin Receptor Blocker HRP and Quinapril in Type 1 Diabetic Rats. Kidney and Blood Pressure Research. 2017;42(1):109-122.
4. Szalay Cs I, Erdélyi K, Kökény G, Lajtár E, Godó M, **Révész C,** Kaucsár T, Kiss N, Sárközy M, Csont T, Krenács T, Szénási G, Pacher P, Hamar P: Oxidative/Nitrative Stress and Inflammation Drive Progression of Doxorubicin-Induced Renal Fibrosis in Rats as Revealed by Comparing a Normal and a Fibrosis-Resistant Rat Strain. PLoS One. 2015;10(6):e0127090.
5. Wasik AA, Koskelainen S, Hyvönen ME, Musante L, Lehtonen E, Koskenniemi K, Tienari J, Vaheri A, Kerjaschki D, Szalay Cs, **Révész C**, Varmanen P, Nyman TA, Hamar P. Holthöfer H, Lehtonen S: Ezrin Is Down-Regulated in Diabetic Kidney Glomeruli and Regulates Actin Reorganization and Glucose Uptake via GLUT1 in Cultured Podocytes. Am J Pathol. 2014;184(6):1727-1739.

6. Kaucsár T, Bodor Cs, Godó M, Szalay Cs I, **Révész C,** Németh Z, Mózes M, Szénási G, Rosivall L, Sőti Cs, Hamar P: LPS-Induced Delayed Preconditioning Is Mediated by Hsp90 and Involves the Heat Shock Response in Mouse Kidney. PLoS One. 2014;19;9(3):e92004.
7. Kaucsár T, **Révész C**, Godó M, Krenács T, Albert M, Szalay Cs I, Rosivall L, Benyó Z, Bátkai S, Thum T, Szénási G, Hamar P: Activation of the miR-17 Family and miR-21 During Murine Kidney Ischemia-Reperfusion Injury. Nucleic Acid Therapeutics, 2013;23(5):344–354.
8. Masszi G, Novák A, Tarszabó R, Horváth EM, Buday A, Ruisanchez E, Tőkés AM, Sára L, Benkő R, Nádasy GL, **Révész C**, Hamar P, Benyó Z, Várbiró Sz: Effects of vitamin D3 derivative--calcitriol on pharmacological reactivity of aortic rings in a rodent PCOS model. Pharmacological reports, 2013;65(2):476-483.
9. Masszi G, Buday A, Novák A, Horváth EM, Tarszabó R, Sára L, **Révész C**, Benkő R, Nádasy GL, Benyó Z, Hamar P, Várbiró Sz: Altered insulin-induced relaxation of aortic rings in a dihydrotestosterone-induced rodent model of polycystic ovary syndrome. Fertility and sterility, 2013;99(2):573-578.
10. Weiszhár Z, Czúcz J, **Révész C**, Rosivall L, Szebeni J, Rozsnyay Z: Complement activation by polyethoxylated pharmaceutical surfactants: Cremophor-EL, Tween-80 and Tween-20. European journal of pharmaceutical sciences: official journal of the European Federation for Pharmaceutical Sciences, 2011;45(4):492-498.
11. Rácz Z, Godó M, **Révész C**, Hamar P.: Immune Activation and Target Organ Damage Are Consequences of Hydrodynamic Treatment but Not Delivery of Naked siRNAs in Mice. Nucl Acid Ther. 2011;21(3):215-224.
12. Fugmann T, Borgia B, **Révész C**, Godó M, Forsblom C, Hamar P, Holthöfer H, Neri D, Roesli C.: Proteomic identification of vanin-1 as a marker of kidney damage in a rat model of type 1 diabetic nephropathy. Kidney Int. 2011;80(3):272-281.
13. Forgács Z, Kubinyi G, Sinay G, Bakos J, Hudák A, Surján A, **Révész C**, Thuróczy G.: 1800 MHz-es GSM-szerű sugárzás hatása hím egerek gonádműködésére és hematológiai paramétereire. [Effects of 1800 MHz GSM-like exposure on the gonadal function and haematological parameters of male mice.] Magy Onkol. 2005;49(2):149-151.

DOI:10.14753/SE.2025.3164

14. **Révész C**, Forgács Z, Lázár P, Mátyás S, Rajczy K, Krizsa F, Bernard A, Gáti I: Effect of Ni^{2+} on primary human ovarian granulosa cells in vitro. Toxicology Mechanisms and Methods. 2004;14(5):287-292.
15. Forgács Z, Somosy Z., **Révész C**, Jánossy G., Thuróczy G: Effect of 50 Hz magnetic field exposure on the adherent cell contacts of primary mouse Leydig cells in culture. Acta Biol Szeged. 2003, 47(1-4): 27-30.
16. Forgács, Z, Némethy, Z, **Révész, C**, Lázár, P.: Specific amino acids moderate the effects of Ni^{2+} on the testosterone production of mouse Leydig cells in vitro. J Toxicol Environ Health, Part A. 2001, 62(5): 349-358.

DOI:10.14753/SE.2025.3164

10. ACKNOWLEDGEMENTS

I want to thank my supervisors, **Prof. Dr. Péter Hamar** and **Dr. Gábor Szénási**, for their dedicated mentorship throughout my PhD studies. Their continuous support and guidance have been essential to my success in my academic pursuits.

I want to express my gratitude to **Prof. Dr. Zoltán Benyó**, the Head of the Institute of Translational Medicine and President of the Doctoral Council, and **Prof. Dr. László Rosivall**, the former Head of the Institute of Pathophysiology and President of the Hungarian Kidney Foundation and the Budapest Nephrology School. The institutions they led and the scientific communities they established provided a supportive environment for my research and facilitated completing my PhD studies.

I thank **Prof. Dr. Attila Mócsai,** the Head of the Department of Physiology, for providing the Mcl1-deleted bone marrow chimeric mice and **Dr. Miklós Kovács** for the bone marrow transplantation.

I am sincerely grateful to all my colleagues, **Dr. Tamás Kaucsár, Mária Godó, Kamilla Kécsán-Révész, and Krisztián Bocskai,** for their kind assistance and valuable advice with the experiments.

Last but not least, I wish to express my appreciation to my family: my wife, **Kamilla**, and my children, **Dorka, Nimród, Dénes,** and **Rozina,** for strengthening my dedication and perseverance during my studies.